AD-A092 362 AIR FORCE INST OF TECH WRIGHT-PATTERSON AFB OH F/G 13/5
FATIGUE IN GRAPHITE/EPOXY BOLTED JOINTS.(U)
JUN 80 M C LEE
UNCLASSIFIED AFIT-CI-80-14T NL

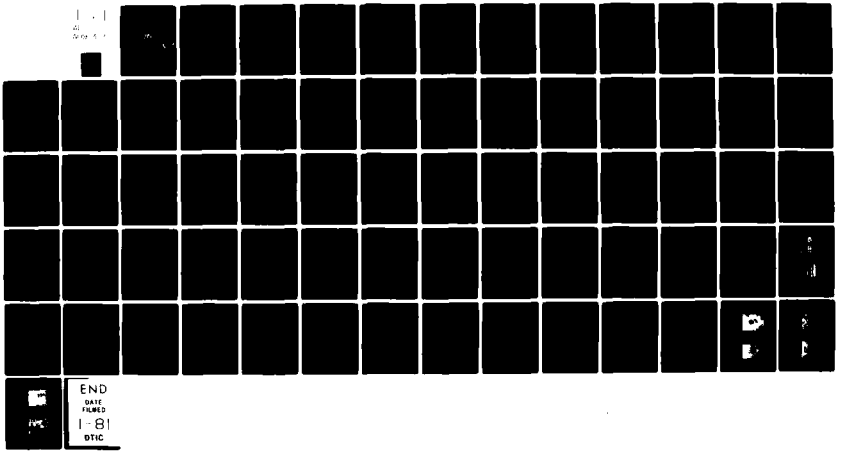

END
DATE FILMED
1-81
DTIC

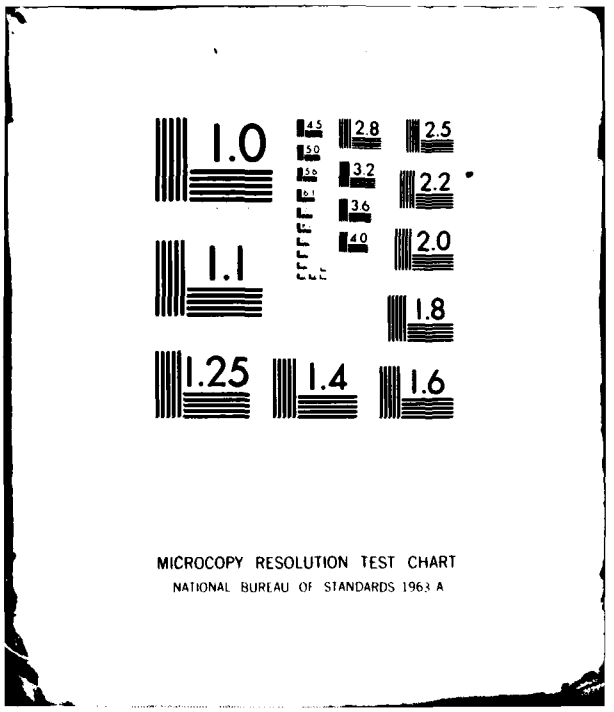
1.0
1.1
1.25
1.4
1.6
1.8
2.0
2.2
2.5
2.8
3.2
3.6
4.0
4.5
5.0
5.6
MICROCOPY RESOLUTION TEST CHART
NATIONAL BUREAU OF STANDARDS 1963 A

AFIT-CI-80-147T

B.S.

UNCLASS

SECURITY CLASSIFICATION OF THIS PAGE (When Data Entered)

AD A092362

REPORT DOCUMENTATION PAGE

READ INSTRUCTIONS BEFORE COMPLETING FORM

1. REPORT NUMBER: 80-14T	2. GOVT ACCESSION NO.: AD-A092362
3. RECIPIENT'S CATALOG NUMBER:	
4. TITLE (and Subtitle): Fatigue in Graphite/Epoxy Bolted Joints	5. TYPE OF REPORT & PERIOD COVERED: THESIS/DISSERTATION
	6. PERFORMING ORG. REPORT NUMBER:
7. AUTHOR(s): Mark Charles Lee, Capt USAF	8. CONTRACT OR GRANT NUMBER(s):
9. PERFORMING ORGANIZATION NAME AND ADDRESS: AFIT STUDENT AT: Massachusetts Institute of Technology	10. PROGRAM ELEMENT, PROJECT, TASK AREA & WORK UNIT NUMBERS: 69
11. CONTROLLING OFFICE NAME AND ADDRESS: AFIT/NR, WPAFB OH 45433	12. REPORT DATE: 11 June 1980
	13. NUMBER OF PAGES: 64
14. MONITORING AGENCY NAME & ADDRESS (if different from Controlling Office)	15. SECURITY CLASS. (of this report): UNCLASS
	15a. DECLASSIFICATION/DOWNGRADING SCHEDULE

LEVEL II

16. DISTRIBUTION STATEMENT (of this Report)

APPROVED FOR PUBLIC RELEASE; DISTRIBUTION UNLIMITED

DTIC ELECTE DEC 3 1980 S D

17. DISTRIBUTION STATEMENT (of the abstract entered in Block 20, if different from Report)

18. SUPPLEMENTARY NOTES

APPROVED FOR PUBLIC RELEASE: IAW AFR 190-17

Air Force Institute of Technology (ATC)
Wright-Patterson AFB, OH 45433

FREDRIC C. LYNCH, Major, USAF
Director of Public Affairs

19. KEY WORDS (Continue on reverse side if necessary and identify by block number)

20. ABSTRACT (Continue on reverse side if necessary and identify by block number)

ATTACHED

DDC FILE COPY

8011 24 060

DD FORM 1 JAN 73 1473 EDITION OF 1 NOV 65 IS OBSOLETE

UNCLASS

SECURITY CLASSIFICATION OF THIS PAGE (When Data Entered)

FATIGUE IN GRAPHITE/EPOXY BOLTED JOINTS

by

MARK CHARLES LEE
Captain, USAF

Master of Science

Massachusetts Institute of Technology
1980

ABSTRACT

Fatigue tests were made on graphite/epoxy bolted joints with an eight ply quasi-isotropic $(90^{\circ}, -45^{\circ}, 0^{\circ}, +45^{\circ})_s$ laminate containing 6.35mm diameter holes. A tensile load was applied to the specimens using a double lap joint configuration with socket head cap screws torqued to 4.0 N-m. Preliminary investigation involved static testing on a range of specimen geometries to determine failure modes, ultimate strengths, and torque effects.

Increasing load (Prot) fatigue tests gave endurance limits as fractions of average static strength were .94 for tension through the hole, .90 for corner shear/shear, and .88 for bearing. The only comparable existing data found was approximately .80 for bearing fatigue.

Thesis Supervisor: Frank A. McClintock

Title: Professor of Mechanical Engineering

FATIGUE IN GRAPHITE/EPOXY BOLTED JOINTS

by

MARK CHARLES LEE

B.S., United States Air Force Academy
(1974)

Submitted in partial fulfillment
of the requirements for the
degree of

MASTER OF SCIENCE

at the

MASSACHUSETTS INSTITUTE OF TECHNOLOGY

June 1980

Signature of Author _____
Department of Mechanical Engineering
May 19, 1980

Certified by _____
Frank A. McClintock
Thesis Supervisor

Accepted by _____
Chairman, Departmental Graduate Committee

ACKNOWLEDGEMENTS

I wish to express my thanks to those who have aided me in this endeavor.

First, to the Air Force Military Personnel Center, that reluctantly changed my assignment allowing me to come to M.I.T. even though they would have rather had me flying O-2s at Shaw AFB, South Carolina. Hopefully this will lead to safer, more effective flying in the future.

Secondly, to Professors Frank A. McClintock and James W. Mar, who gave me the guidance necessary to complete this project.

Finally, to all those who aided in specimen fabrication and testing: Albert T. Supple, Jr. with his testing machine; Fred Merlis and his strain gages; Earl Massmouth's help with cutting and drilling; Jose Garcia's aid in specimen curing; and John Roman at Grumman Aerospace for assistance in torque selection.

This work was supported by the Air Force Office of Scientific Research under Contract No. F49620-80-C0010. Lt Col Joseph D. Morgan III is the contract supervisor.

80-14T

AFIT RESEARCH ASSESSMENT

The purpose of this questionnaire is to ascertain the value and/or contribution of research accomplished by students or faculty of the Air Force Institute of Technology (ATC). It would be greatly appreciated if you would complete the following questionnaire and return it to:

AFIT/NR
Wright-Patterson AFB OH 45433

Research Title: Fatigue in Graphite/Epoxy Bolted Joints

Author: Capt Mark Charles Lee

Research Assessment Questions:

1. Did this research contribute to a current Air Force project?

a. Yes b. No

2. Do you believe this research topic is significant enough that it would have been researched (or contracted) by your organization or another agency if AFIT had not?

a. Yes b. No

3. The benefits of AFIT research can often be expressed by the equivalent value that your agency achieved/received by virtue of AFIT performing the research. Can you estimate what this research would have cost if it had been accomplished under contract or if it had been done in-house in terms of manpower and/or dollars?

a. Man-years _____. b. $_____

4. Often it is not possible to attach equivalent dollar values to research, although the results of the research may, in fact, be important. Whether or not you were able to establish an equivalent value for this research (3 above), what is your estimate of its significance?

a. Highly Significant b. Significant c. Slightly Significant d. Of No Significance

5. AFIT welcomes any further comments you may have on the above questions, or any additional details concerning the current application, future potential, or other value of this research. Please use the back of this questionnaire for your statement(s).

NAME GRADE POSITION

ORGANIZATION LOCATION

USAF SCN 75-208

TABLE OF CONTENTS

TABLE OF CONTENTS (Continued)

LIST OF FIGURES

LIST OF TABLES

LIST OF SYMBOLS

E_L - Longitudinal Modulus

E_T - Transverse Modulus

G_{LT} - Longitudinal-transverse shear modulus

ν_{LT} - Major Poisson's Ratio

V_f - Fiber Volume Fraction

E_x - Modulus in 0° laminate direction

E_y - Modulus in 90° laminate direction

ν_{xy} - Major Poisson's Ratio

ν_{yx} - Minor Poisson's Ratio

$$\epsilon_x = \frac{\sigma_x}{E_x} - \frac{\sigma_y \nu_{yx}}{E_y}$$

1. INTRODUCTION

At an ever increasing rate, advanced fiber reinforced composite materials are being used by the aerospace industry in space and airframe structures. Several features of these materials make them particularly suited to this industry:

i) Weight savings

ii) Anisotropic strength

iii) High fatigue to tensile strength

iv) High damage tolerance.

As composite components become larger and more numerous, so do the problems of joining them to structural members and each other, whether by bonding or mechanical fasteners. While bonded joints are stronger, lighter, and have less stress concentration, they require surface preparation, are susceptible to climatic degradation, cannot be disassembled, and are difficult to inspect. Mechanically fastened joints in composite materials, while easier to assemble, inspect, and repair, require machining of holes and create stress concentrations at the bearing surface.

Very little work has been done on bolted joints, even though they have proven to be both structurally efficient and necessary. Literature on static loading has only originated within the past few years and ranges from joint design for specific applications, such as the space

shuttle (1), to simple joints (2), to comprehensive test programs for multi-bolt joint design (3). The only information found to date on bolted joint fatigue (4) provides S-N bearing data for several different layups in a single lap joint, but is clearly only the beginning. For the dynamic environment that these structures will experience, fatigue must be taken into consideration. Hopefully, the increasing load (Prot) fatigue methods discussed here will prove to be reliable and expedite research efforts.

2. THE EXPERIMENT

2.1 Laminate Selection

Since the possible fiber patterns in composites are unlimited, a layup that has proven effective in increasing bolted joint strength was selected from the quasi-isotropic group. Although high matrix stresses occur when numerous adjacent plies are in parallel orientation, this layup $(90^{\circ}, -45^{\circ}, 0^{\circ}, +45^{\circ})_s$ rotates successive about the symmetric centerline to obtain a uniform dispersion of fiber directions. Although this is ideal for joint design, it does not allow orienting fibers to maximize strength and stiffness. Other methods are being tested to aid these more unidirectional composites such as adding Mylar film or extra plies or routing glass or Kevlar fibers around the bolt hole. Although some fabrication difficulties are associated, they show great promise and are subjects of continuing investigation.

2.2 Specimen Preparation

2.2.1 Material

Hercules type AS 3501/6 pre-impregnated graphite/epoxy tape was used for this study. Conventional techniques were used in the layup, autoclave curing, and

bonding of the laminates. A complete description of these procedures is given in Appendix A. Six 300mm by 350mm sheets were cured at a time in each of three separate cures. Specimen panels were cut from the larger sheets and holes drilled, using diamond studded saw blades and drill bits with water cooling. There was no visual evidence of any defects associated with the cutting and drilling process.

2.2.2 Glass/Epoxy Loading Tabs

Eight ply $(0^{\circ}_2/90^{\circ}_2)$s thick glass/epoxy, type 3M SP-1002, was used for the loading tabs, which were bonded to the graphite/epoxy panels with American Cyanide FM 123-2 adhesive film.

2.2.3 Design

Specimens were designed so that multiple data points could be obtained from the same panel, which significantly reduced the amount of material needed and the fabrication time. Figure 1 shows a typical static test specimen. After the outer hole was tested (A), a section was cut off 30mm above the center of that hole. A new hole (B) was then drilled, tested, and the process repeated (C) giving three data points from each specimen.

2.3 Specimen Dimensions and Nomenclature

The width (w) and edge distance (e), measured from hole center to end of panel, will be given as the ratios (w/d) and (e/d), respectively, where (d) is the 6.35mm hole diameter.

2.4 Loading Fixture

Several types of loading fixtures were built in an effort to detect damage in the specimen between the two loading plates in a double lap joint configuration. Attempts to use ultrasonic reflected transmissions were unsuccessful and although ultrasonic through transmissions have been successful in the past (5), the required dismantling of the loading fixture to use this method would have itself contributed to fatigue. Since damage initiation was primarily of interest in fatigue testing, a simple steel loading fixture (Figure 2) was used for the static tests. Fortunately, the brittle nature of failure permits some damage detection from plots of load versus crosshead displacement and will be discussed in Section 4.4.

To observe damage visually during fatigue testing, a fixture was designed using clear plexiglass plates. Although this fixture seemed promising, the plexiglass is too soft and the deforming graphite/epoxy caused

indentations which effectively reduced the clamping force and made observation of the laminate difficult after only two tests. Therefore, the steel loading fixture was also used for fatigue testing.

2.5 Bolts and Torque Selection

Alloy steel socket head cap screws with a tensile strength of 1310 MPa were used. A new screw and nut were used for each test to reduce bolt distortion and maintain as uniform a bolt clamping force between tests as possible.

Several factors were considered in selection of the torque for this test: transverse crushing strength of specimen, maximum bolt torque, practical values in use today, and those used in other studies.

While the crushing strength allows a torque of 60 N-m (Appendix B) and the maximum bolt torque is 27 N-m (6), most data is in the 3.0 N-m area. Even though several sources report their torque as being, "common for composite application", the torque is not so much a function of the composite material in use as the joint configuration. Consultation with John Roman at the Grumman Aerospace Corporation revealed that special torque values are not given to joints just because composites are used and he recommended a value between 3.4 - 4.5 N-m

for a double lap joint configuration. Therefore, a value of 4.0 N-m was selected for these tests.

3. STATIC TESTING

3.1 Objectives

Although data are available on strengths and failure modes of double lap bolted joints, there were enough differences in required layup, torque, and thickness to require a separate test program. A total of eighty specimens were tested, with a range of width and edge distance combinations, to determine those geometries that would be tested under cyclic loading. Basic laminate and joint static strengths were needed for determination of joint efficiencies and comparison with the endurance limits from Prot fatigue testing.

3.2 Basic Laminate

Five specimens were tested to determine the material properties of the laminate without a hole. The monolayer and experimentally determined laminate properties are shown below:

Monolayer Properties

t_{ply}	= 135mm	G_{LT}	= 6.0 GPa
E_L	= 130 GPa	ν_{LT}	= .28
E_T	= 10.5 GPa	V_f	= .60

Experimental Laminate Properties

t_{ply}	= 137mm Ave.	G	= 18 GPa
E_x	= 48 GPa	ν_{xy}	= .28
E_y	= 45 GPa	ν_{yx}	= .24
F_x^{tu}	= 486 MPa	F_{xy}^{su}	= 320 MPa

3.3 Joint Efficiency Analysis

Joint efficiency, η, is defined as the ratio of failure load, P, to the unnotched laminate ultimate tensile strength, F_x^{tu}, times the gross section area,

$$\eta = \frac{P}{F_x^{tu} wt.} \qquad (1)$$

Data from static testing is presented in Figure 3 as the variation in joint efficiency with width (w/d) and edge distance (e/d). Since three specimens were tested at each geometry, they were averaged and plotted as one point. The relationship of joint efficiency to joint geometry is given by writing Eq (1) for the various failure modes as a function of stress concentration factors (tension - c_t, shear - c_s, bearing - c_b) and ultimate laminate strengths (tension - F_x^{tu}, shear - F_{xy}^{su}, bearing - F^{br}) as,

Tension $$\eta_t = \frac{(F_x^{tu}/c_t)(w-d)t}{F_x^{tu}\,wt} = \frac{(1-d/w)}{c_t} \quad (2)$$

Shear $$\eta_s = \frac{(F_{xy}^{su}/c_s)(2et)}{F_x^{tu}wt} = \frac{2F_{xy}^{su}ed}{F_x^{tu}c_s dw} \quad (3)$$

Bearing $$\eta_b = \frac{(F^{br}/c_b)(dt)}{F_x^{tu}wt} = \frac{F^{br}d}{F_x^{tu}c_b w.} \quad (4)$$

They show the expected dependence of tension and bearing on width, while shear is a function of edge distance at any particular width. Equations (2 - 4) can be further reduced by calculating the actual stress concentration factors encountered during these tests, $c_b = 1$ $C_s = 1.5$ $c_t = 1.45$, and substituting values for the ratios of laminate shear and bearing strength to tensile strength, $F_{xy}^{su}/F_x^{tu} = .67$ $F^{br}/F_x^{tu} = 2$. While the stress concentration factors are average values based on just a few tests, the actual values do not vary much over the range of geometries studies. The results are:

$$\eta_t = \frac{(1-d/w)}{1.45} \quad (5)$$

$$\eta_s = .95(e/d)(d/w) \quad (6)$$

$$\eta_b = 2d/w. \quad (7)$$

These equations are indicated on Figure 3 and show lines along which the respective type of failure (Figure 4) would predominate if there was no transition between modes. If stress concentration factors are known beforehand, both the expected failure mode and load can be determined for a particular joint geometry. Although it is not possible to determine which mode will predominate in a transition area, the area itself can be determined by equating joint efficiencies.

3.4 Selection for Fatigue Study

On the basis of the static tests, four geometries were selected for fatigue study because they represented tension, shear, corner shear, and bearing failure. These four modes provide a basis on which the Prot method can be evaluated.

Corner shear, while not one of the more basic failure patterns, was selected because it was shear strength critical but did not exhibit the same failure surface as shear. Probably a better description would be corner tearout. It will be tested and presented in the same group as the shear specimens because of the identical shear failure strengths. Those geometries selected are shown below:

i) Tension - $w/d = 4$ $e/d = 4$ $\mu = .5$

Average ultimate strength - 320 MPa

ii) Shear - w/d = 8 e/d = 2 μ = .22

Corner Shear - w/d = 5 e/d = 2 μ = .24

Average ultimate strength - 220 MPa

iii) Bearing - w/d = 8 e/d = 8 μ = .24

Average ultimate strength - 960 MPa

3.5 Pin Loading

Every geometry was also tested with pin loading to determine the effect of clamping force. Regardless of width and edge distance, failure was by bearing. Figure 5 shows testing computer plots for the 4.0 N-m and 0 N-m torque values and demonstrates the impact that clamping force has on failure load. Average reductions in yield and ultimate bearing strengths were 40 and 55 percent, respectively.

4. FATIGUE TESTING

4.1 Objective

To develop a program for fatigue testing using the Prot method and establish endurance limits for the three basic failure modes: tension, shear/corner shear, and bearing.

4.2 The Prot Method

The Prot method has proven to be effective in ferrous metals for providing an estimate of the endurance limit from a minimum number of tests (7). It is based on the assumption that a linear relationship exists between the fatigue failure stress, σ_f, endurance limit, σ_e, and the square root of the load increase per cycle, x,

$$\sigma_f = \sigma_e + k\sqrt{x}. \qquad (8)$$

The advantage of this method is that every specimen breaks and contributes to the endurance limit estimate, so fewer specimens are necessary. An assumption of the Prot method is that an endurance limit exists, and cycles of stress below this level cause no damaging or strengthening effect in the material. Therefore, the stress at which loading is initiated will not affect the results as long as it is

below the endurance limit. The continuously increasing load was simulated by 30 - 40 step increases, depending on specimen life, with 1,800, 7,200, and 27,000 cycles/step for tension and shear/corner shear and 3,600, 18,000, and 36,000 cycles/step for bearing.

4.3 SF-1U Fatigue Machine

4.3.1 Loading Apparatus

The SF-1U operates at a constant 30 Hz with a preset mechanical oscillating load and automatic, but adjustable, static force controller. Because of the change from the hydraulic grip static test machine to the fatigue loading fixture (Fig 6), specimens (Fig 7) had to be altered to allow a pin connection through the loading tabs and limited each specimen to one data point due to length. The machine produced reliable results and is particularly suited to stiff materials such as graphite/epoxy.

4.3.2 Test Procedures

Loading was initiated after insuring the bolted joint and pinned loading connection were in line. Initial maximum stress was selected as 50 percent of the respective failure strength and the minimum to produce

a mean load ratio, R = σ_{max} / σ_{min}, of .1. Loads were added while cycling using the automatic static force controller. Since this load increases both the maximum and minimum stress, a constant R value could not be obtained. Once each test reached 75 percent of static strength, the oscillating load was stopped and it, along with the static load, was adjusted to return R to .1. The initial stress increase rate was chosen so the test would take approximately 10^6 cycles to go from 50 to 100 percent of static failure strength in one percent step increases. Faster rates were then chosen for a broad range of values.

4.4 Damage Detection

Analysis of the load versus crosshead displacement plots (Fig 8) from static testing showed a significant load dropoff at bearing yield while only a series of small load reductions preceded failures by tension, shear, or corner shear. The automatic static load controller was sensitive enough to correct for the small load reductions and gave a reliable forecast of failure while bearing yield was clearly indicated by continuous operation of static load control for approximately five seconds.

4.5 Endurance Limits and Statistical Analysis

Results of the Prot fatigue testing are shown in Figures 9 - 11. A least squares line is drawn through the data by eye and extrapolation back to zero rate of load increase produces the desired best estimate of the endurance limit. Reductions in strength, as fractions of average static strength, by this method ranged from .06 for tension, to .1 for shear/corner shear, and .12 for bearing.

Since scatter is inherent for fiber composites, we must now predict a lower limit for the stress which would cause failure of the next specimen at zero rate of load increase. The regression analysis described in reference 8 can easily be applied in this case and a quick approximation made. For a confidence factor of 95 percent and the number of specimens in this test, the 95 percent lower limit will be below the endurance limit by about twice the standard deviation of the stress levels. Since the standard deviation for a normal distribution is that distance on each side of the least squares line which encompasses tow-thirds of the sample, the lower 95 percent prediction limit can be simply estimated by eye.

5. CONCLUSIONS AND RECOMMENDATIONS

Although there is limited conventional data for comparison, the endurance limits obtained from the Prot method are approximately 10 per cent higher. A slight increase in endurance limits for metals was also indicated using this method (7), but the inability to maintain a constant R value also contributed. While data used for comparison (4) was all gathered with an R value of .05, a range of .1 - .3 could only be met by this test program. Using the Prot method under identical test conditions could continue to show this procedure as reliable as conventional techniques. This method is also suited to specialized joint configurations where an endurance limit could be obtained from a limited number of tests.

An interesting aspect of designing for fatigue is the amount of scatter obtained in testing. In these tests, the strength reduction to obtain the endurance limit is not as large as that associated with obtaining the 95 per-cent confidence limit. Until more information is available, a high safety factor must be employed.

Clamping force is extremely critical in composites because of the reduction in bearing yield strength for pinned connections. This is before consideration of fatigue, which would cause further reductions. While torque lock nuts do not ensure a constant clamping force,

they are probably the most practical means of solving this problem.

Use of the joint efficiency equations makes it possible to obtain rough estimates of failure data if good approximations of the stress concentration factors can be made.

The results of this test and desirable characteristics of the Prot method warrant further study. If the increasing load method can be shown to be as reliable as conventional testing, the time savings will be significant.

REFERENCES

1. Design Fabrication and Test of Graphite/Polyimide Composite Joints and Attachments for Advanced Aerospace Vehicles, National Aeronautics and Space Administration Report No. NASA-CR-159080; QTPR-1, April, 1979

2. Collings, T.A., "The Strength of Bolted Joints In Multi-Directional CFRP Laminates," Composites, Vol. 8, January, 1977, pp. 43-55.

3. Hart-Smith, L.J., "Bolted Joints in Graphite/Epoxy Composites, National Aeronautics and Space Administration Report No. NASA-CR-144899, June, 1976.

4. Engineering Design Handbook: Joining of Advanced Composites, DARCOM Pamphlet No. 706-316, March, 1979.

5. Maass, D.P., "The Effects of Compression Fatigue on Failure Modes of Graphite/Epoxy Laminates," M.I.T., Department of Aeronautics and Astronautics, S.M. Thesis, September, 1977.

6. Unbrako Socket Screws, SPS Technologies, Jenkintown, Pennsylvania, 1978.

7. Corten, H.T., Dimoff, T., Dolar, T.J., "An Appraisal of the Prot Method of Fatigue Testing," American Society for Testing Materials Proceedings, Vol. 54, 1954, pp. 875-902.

8. McClintock, F.A., "The Statistical Planning and Interpretation of Fatigue Tests," Metal Fatigue, McGraw-Hill Book Company, Inc., New York, 1959, pp. 112-141.

9. Timoshenko, S., Strength of Materials, D. Van Nostrand Co., Inc., Princeton, New Jersey, 1956, p. 1.

REFERENCES (Continued)

10. Wilkins, D.J., "Environmental Sensitivity Tests of Graphite Epoxy Bolt Bearing Properties," Composite Materials: Testing and Design (Fourth Conference), ASTM STP 617, American Society for Testing and Materials, 1977, pp. 497-513.

11. Tsai, S.W., Hahn, H.T., Introduction to Composite Materials Volume I: Deformation of Unidirectional and Laminated Composites, Air Force Materials Lab Technical Report 78-201, January, 1979.

12. Whitney, J.M., and Nuismer, R.J., "Stress Fracture Criteria for Laminated Composites Containing Stress Concentrations," Journal of Composite Materials, Vol. 8, July, 1974, pp. 253-265.

13. Hashin, Z., and Rotem, A., "A Fatigue Failure Criterion for Fiber Reinforced Materials," Journal of Composite Materials, Vol. 7, October, 1973, pp. 448-464.

14. Waszczak, J.P., and Cruse, T.A., "Failure Mode and Strength Predictions of Anisotropic Bolt Bearing Specimens," Journal of Composite Materials, Vol. 5, July, 1971, pp. 421-425.

15. Dastin, S.J., "Joint Designed Fiber Glass Reinforced Aircraft Composites," American Society of Mechanical Engineers, Paper No. 70-DE-65, May, 1970.

16. Siegel, M.J., Maleev, V.L., Hartmah, J.B., Mechanical Design of Machines, International Textbook Co., Scranton, Pennsylvania, 1965, p. 300.

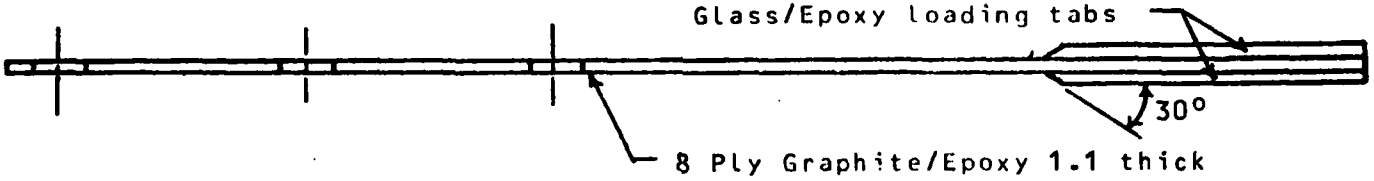

Widths (w/d) of 3, 4, 5, 6 for Tension; 8 for Bearing and Shear

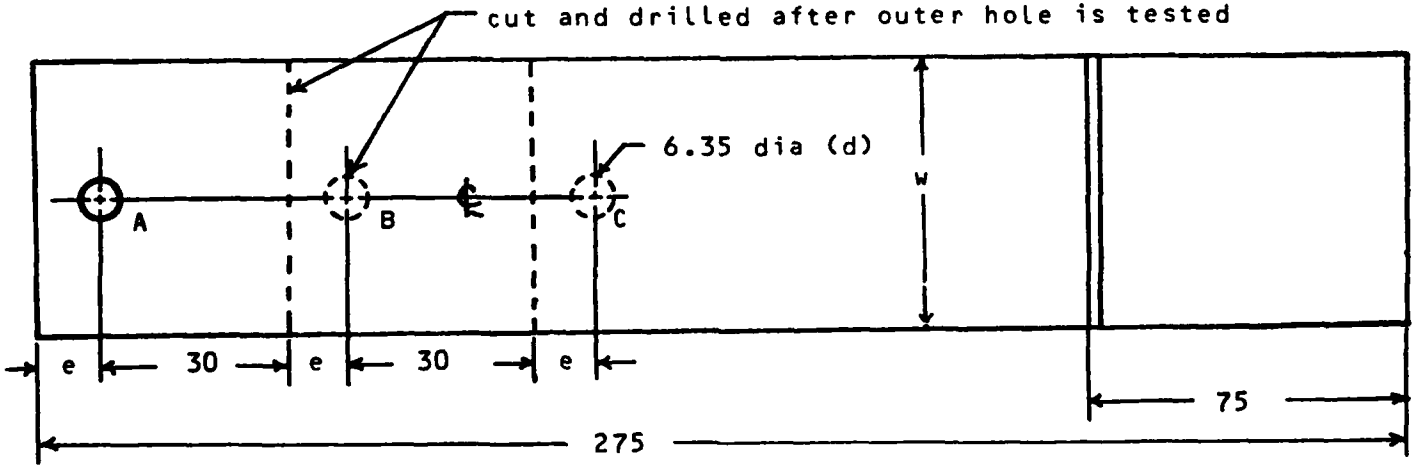

Edge distance (e/d) of 2, 4, 6 for Tension; 2, 3, 4, 8 for Bearing and Shear

All dimensions in mm

Figure 1. Static test specimen

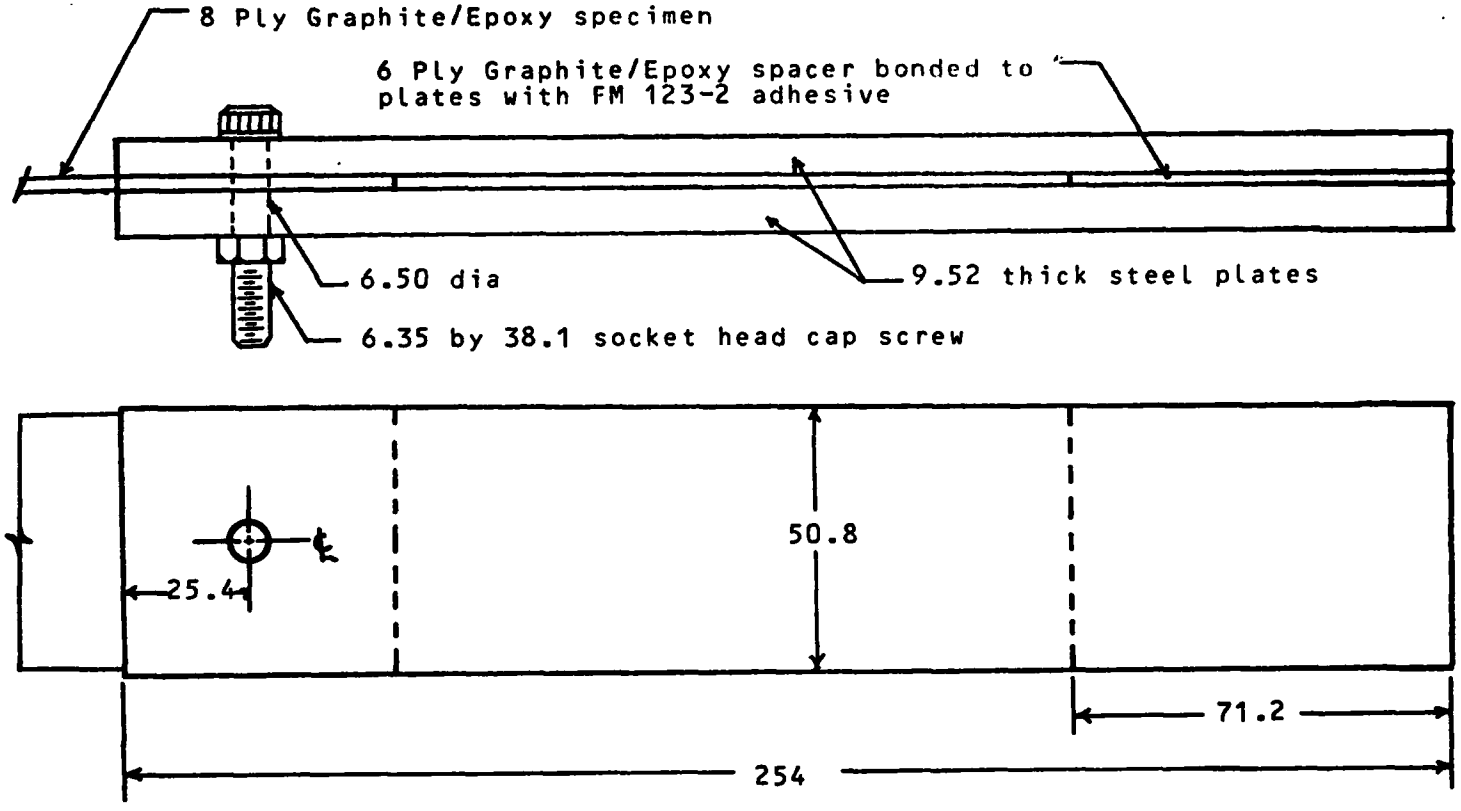

All dimensions in mm.

Figure 2. Steel loading fixture

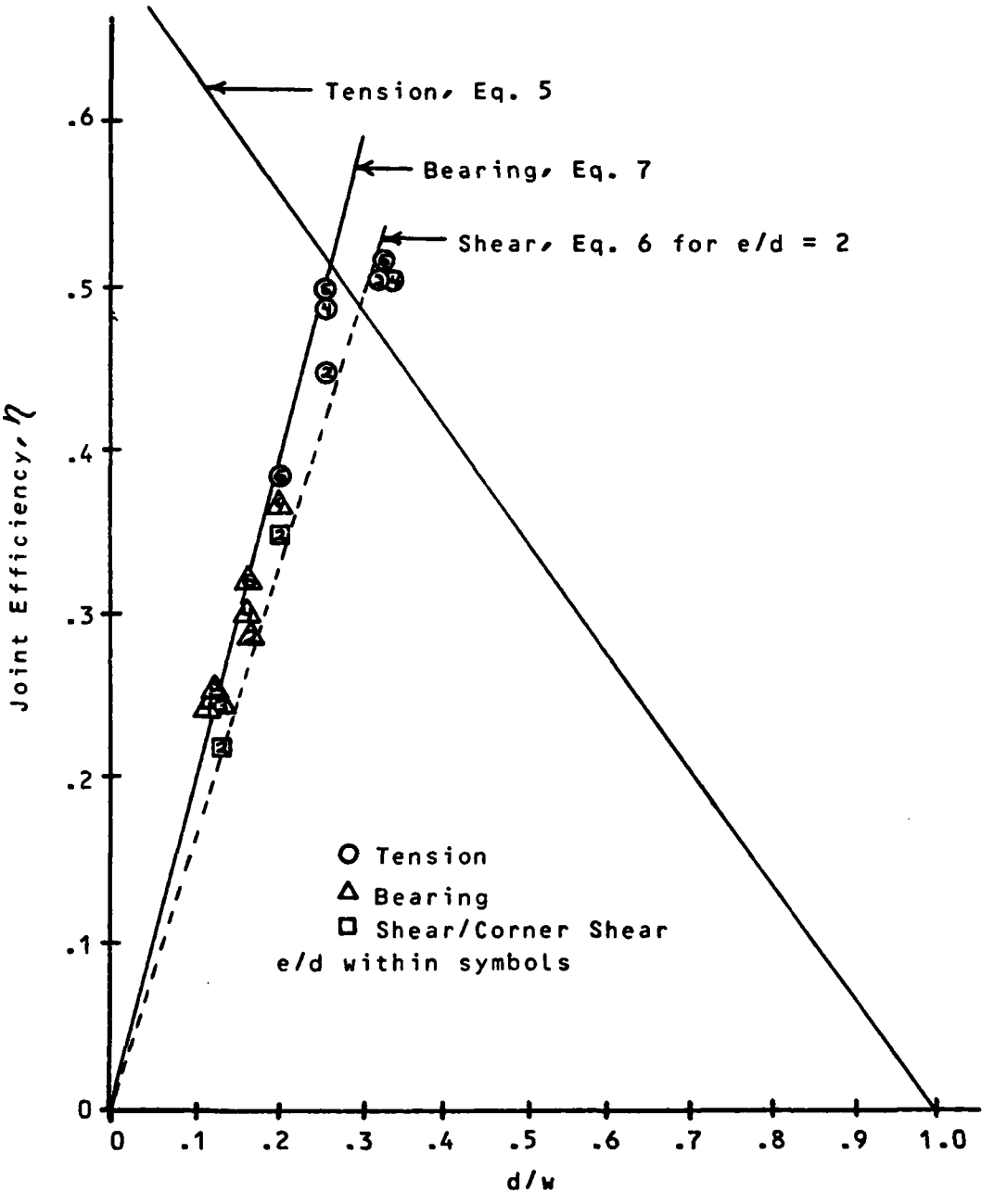

Figure 3. Failure modes as a function of joint geometry

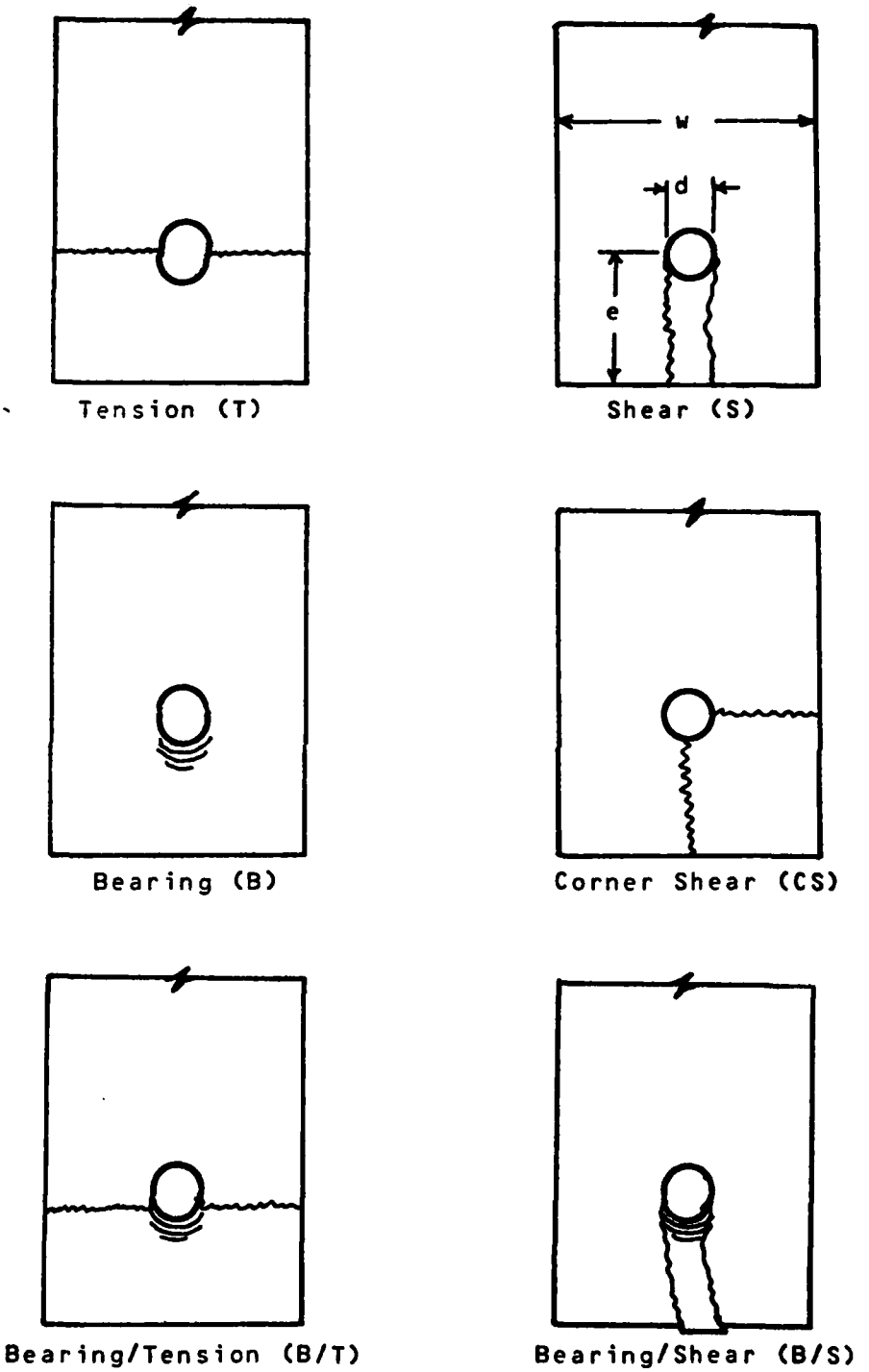

Figure 4. Typical failure modes

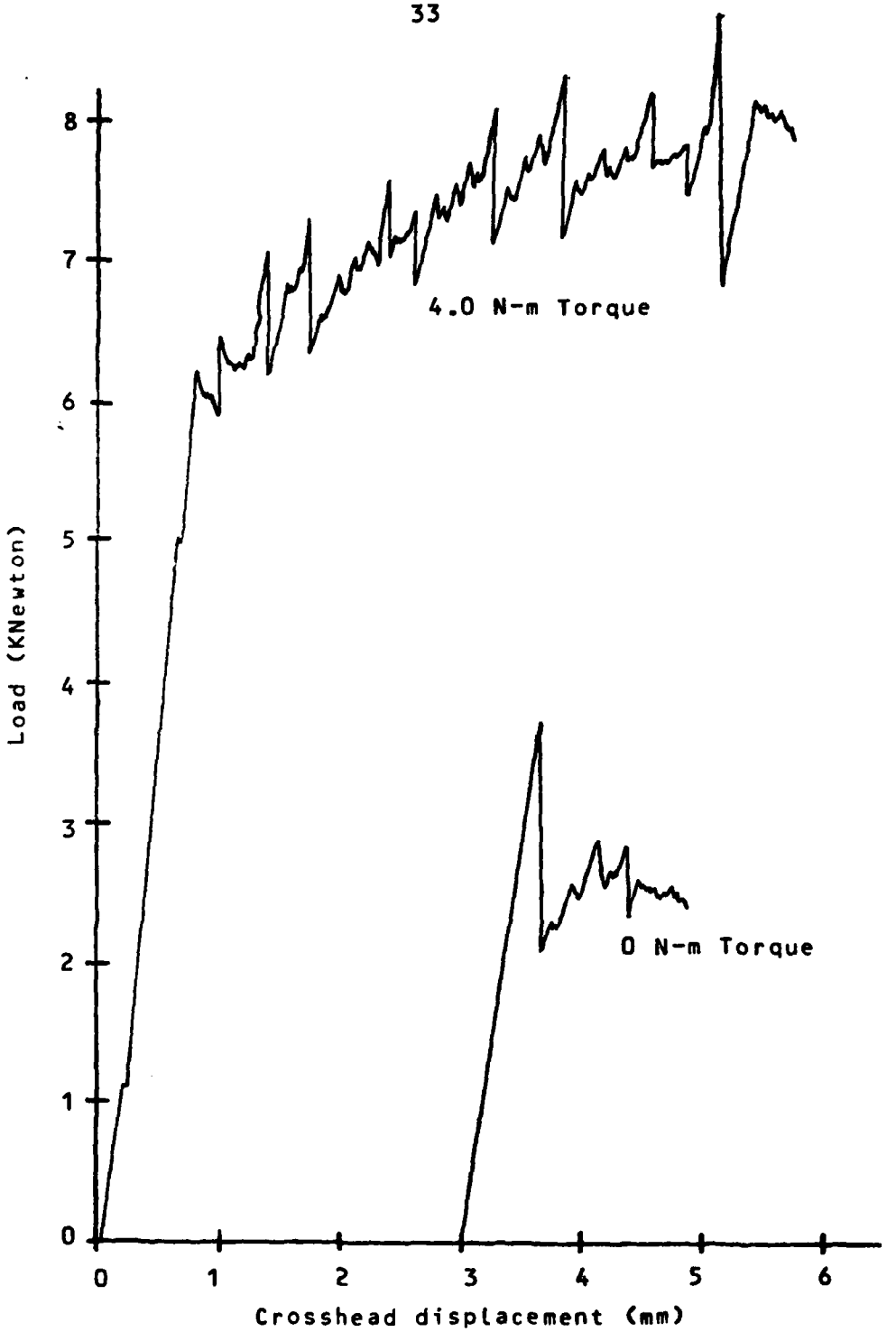

Figure 5. Variation of load with clamping force for bearing critical specimens

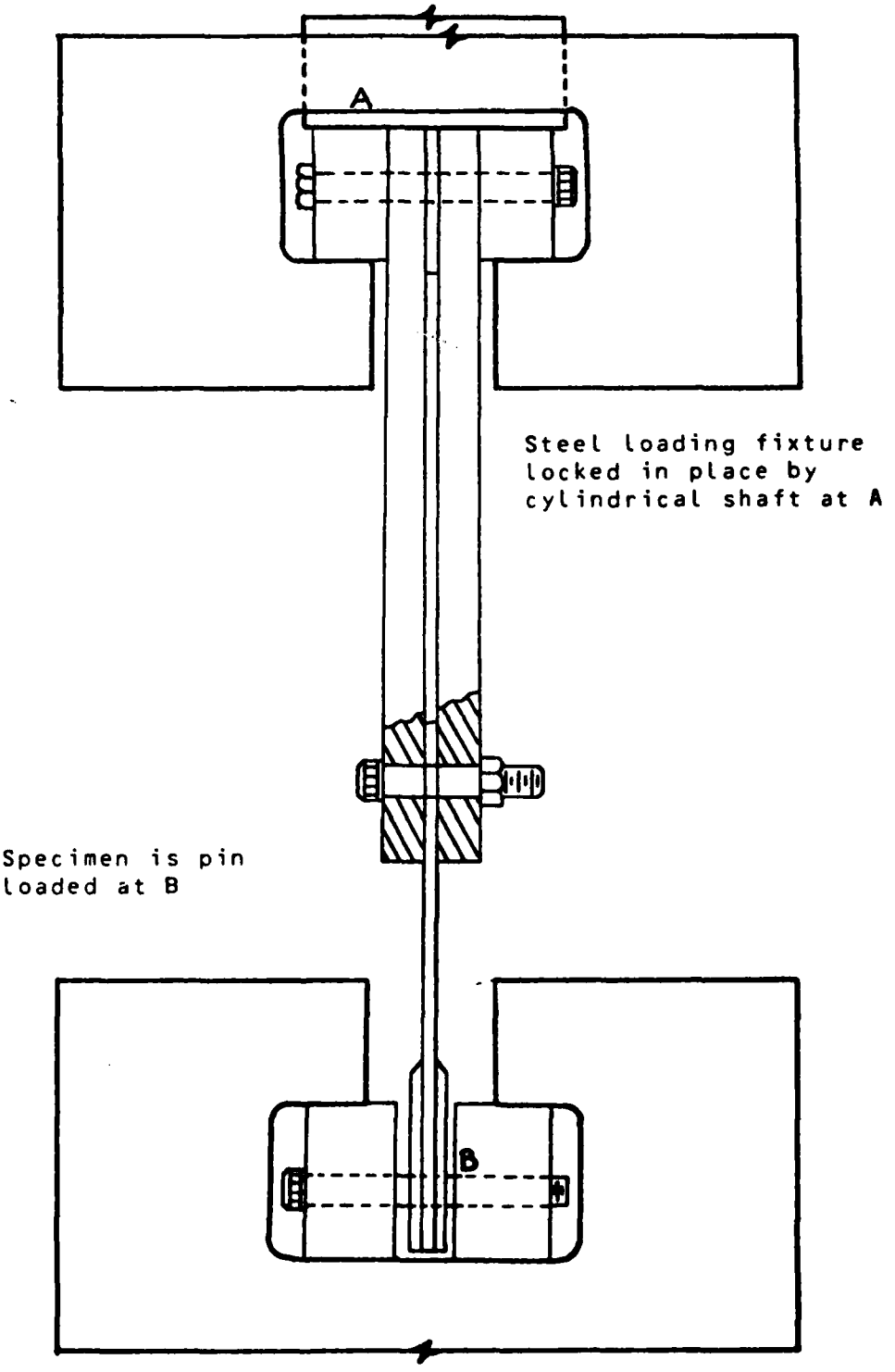

Figure 6. Fatigue Loading Grips

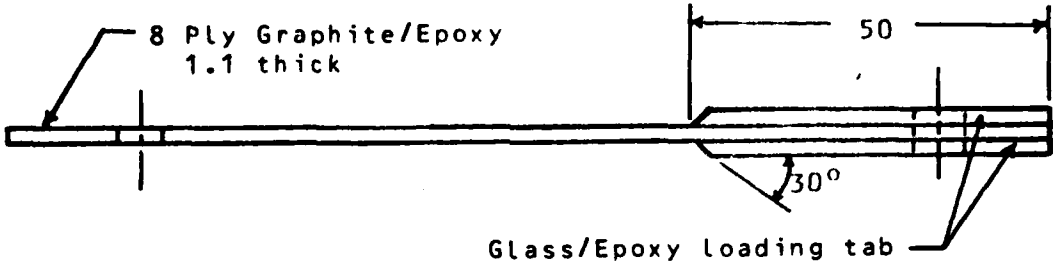

Width (w/d) of 4-Tension; 5-Corner Shear; 8-Shear and Bearing

Edge distance (e/d) of 4-Tension; 8-Bearing; 2-Corner Shear and Shear

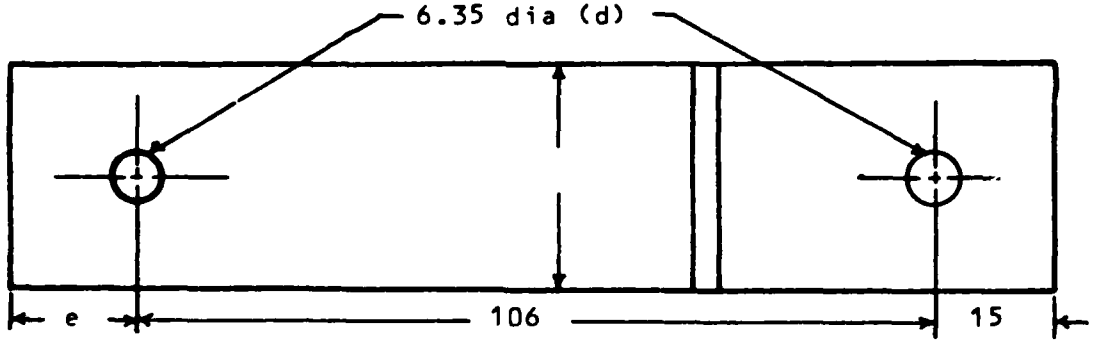

All dimensions in mm

Figure 7. Fatigue specimen

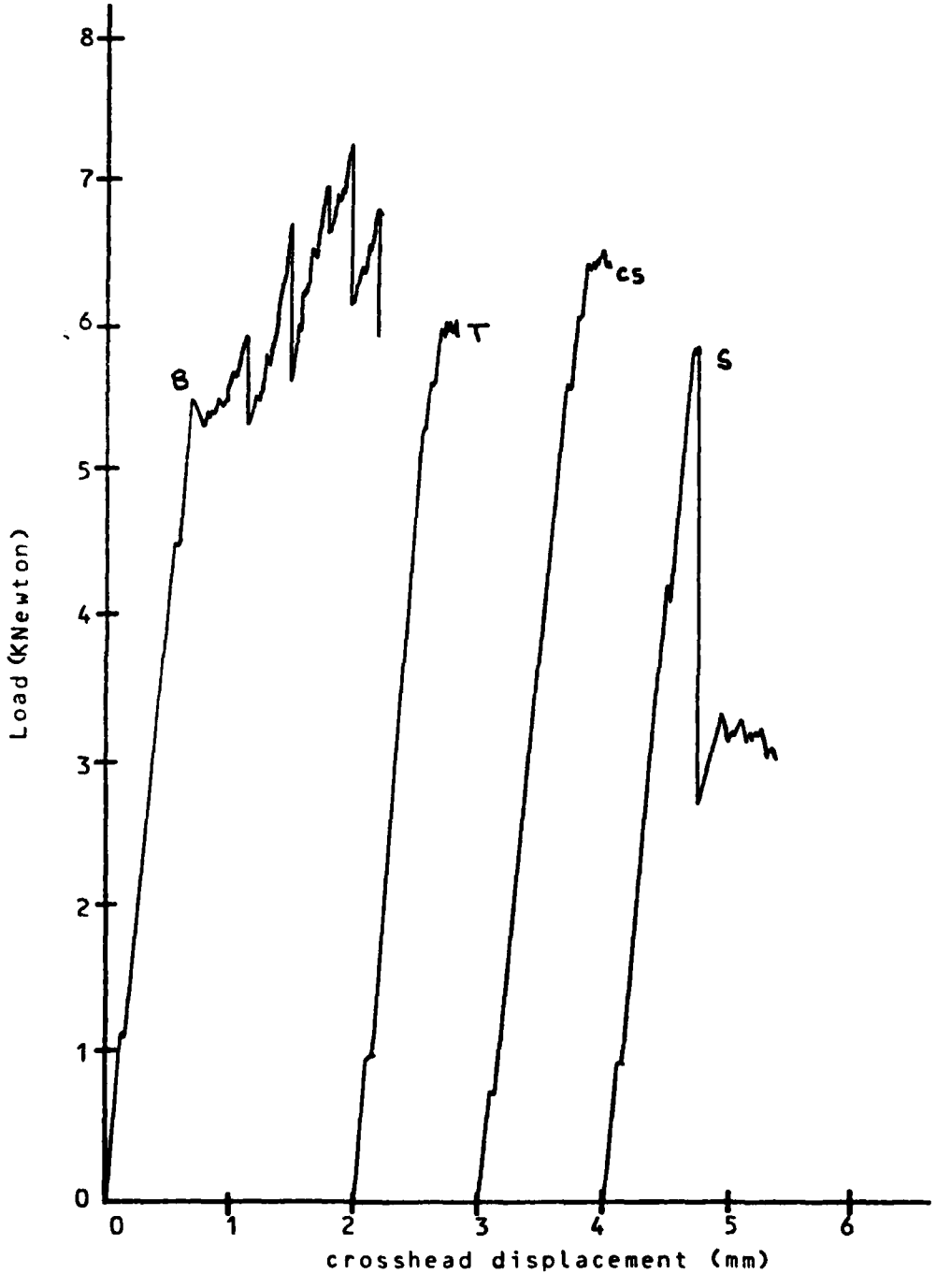

Figure 8. Static load vs. crosshead displacement

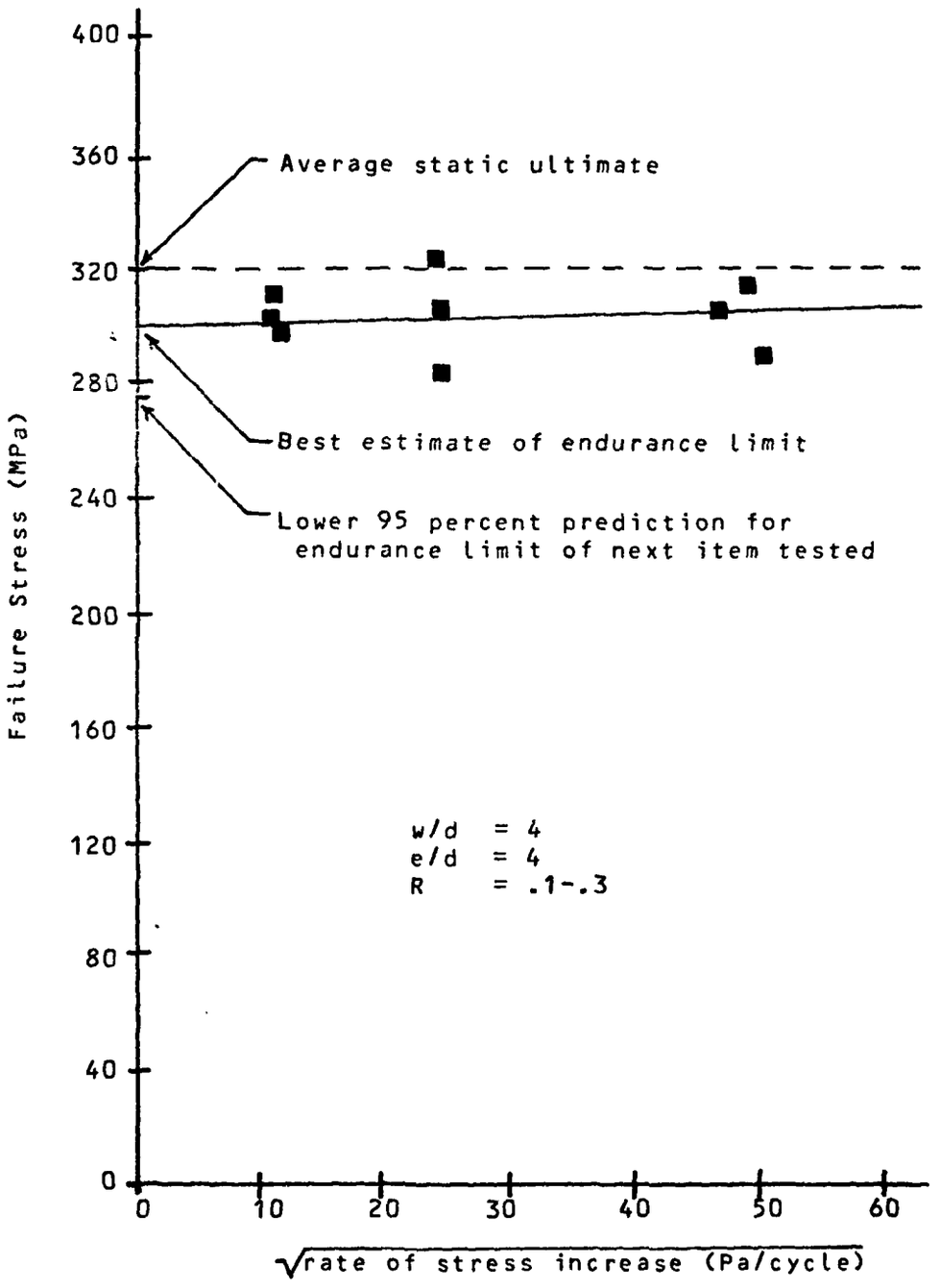

Figure 9. Prot fatigue data - Tension failure

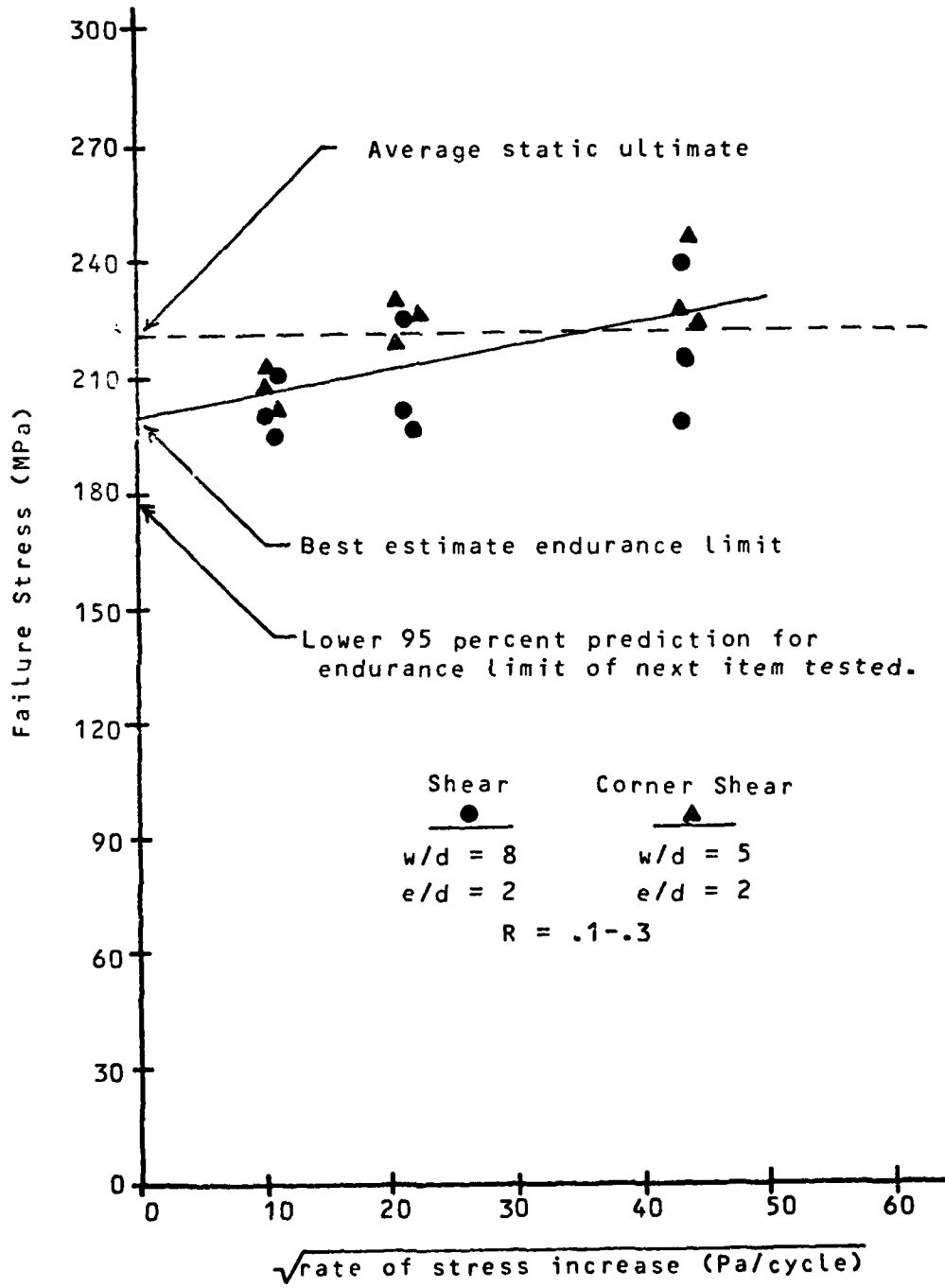

Figure 10. Prot fatigue data - Shear/Corner Shear failure

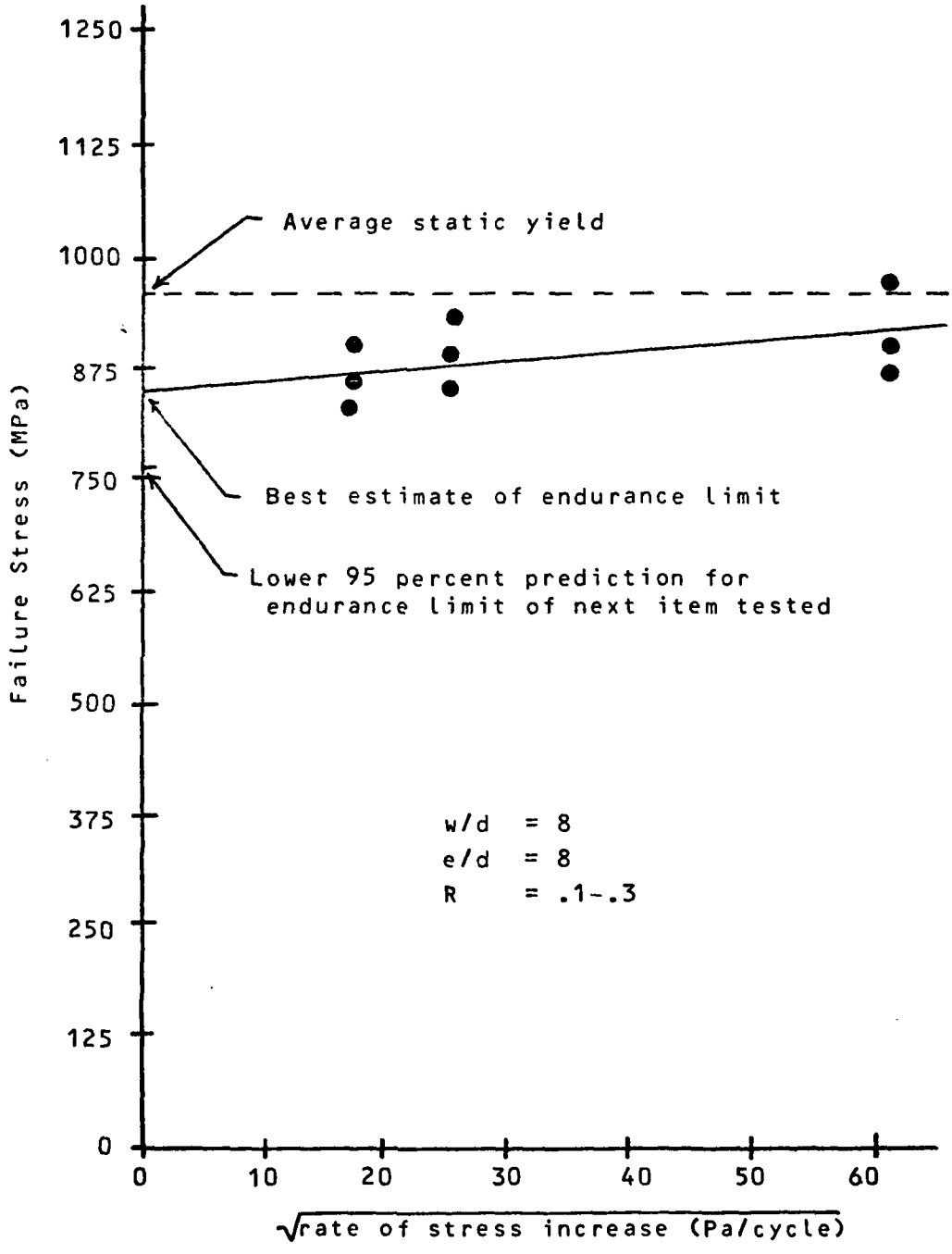

Figure 11. Prot fatigue data - Bearing failure

APPENDIX A

CURING AND FABRICATION PROCEDURES

A.1 Graphite/Epoxy

Individual plies were cut from the 300mm by 30m rolls using templates and X-Acto knives. These plies were then laid-up in the appropriate sequence (90^{o}, -45^{o}, 0^{o}, $+45^{o}$, $+45^{o}$, 0^{o}, -45^{o}, 90^{o}) to form 300mm by 350mm sheets of uncured laminate. Angles are measured from the longitudinal axis, with clockwise positive.

A fabric peel ply was then put on each side of the laminate which allows excess resin to escape during cure. The other materials and layup required for the curing process are shown in Figure A1. One sheet of paper resin bleeder is used for each two plies in the laminate and is the only part of the layup that would change as the number of plies in the laminate is increased.

Six laminates were cured at one time in an autoclave using the cure cycle shown in Figure A2, and the entire assembly was allowed to cool to room temperature before dismantling. The laminates were then post cured in an oven for eight hours at 350^{o} F.

The graphite/epoxy was cut into strips on a milling machine using a water-cooled diamond blade at a speed of 9 3/4 in/min. To avoid any damage to the laminate, the peel ply was not removed until after cutting.

Holes were drilled in the graphite/epoxy using a flat head diamond studded drill (6.10mm dia) and reamer (6.35 mm dia) set. In several cases, delamination of the 90° fibers on the bottom of the specimen ocurred due to lifting the graphite/epoxy panel during the drilling process. These specimens were discarded, but in all cases that the drill was allowed to completely go through the laminate prior to moving it, a high quality hole was obtained with no visible defects.

A.2 Glass/Epoxy Loading Tabs

The glass/epoxy is cut from 300mm wide rolls and laid-up eight plies thick $(0^{\circ}_2/90^{\circ}_2)$s to form 300mm square sheets. The curing layup is shown in Figure A3 and curing was accomplished at 340° F for two hours (no heat up or cool down rates specified) with a pressure of 25 psig and vacuum set at 28 in Hg. Loading tabs are cut from the large sheet, 15 1/2 in/min, with a water-cooled diamond blade. Tabs are 75mm long and 4mm wider than the graphite/epoxy specimen that they will be bonded to. One edge of the tab is beveled at 30° to the plane of the specimen to help relieve the stress concentration at the bond edge (4).

A.3 Bonding of Glass/Epoxy Tabs to Graphite/Epoxy

Adhesive film, American Cyanide FM 123-2, was used to bond the glass/epoxy tabs to the graphite/epoxy specimens. The adhesive film was cut slightly larger than the loading tab and requires care in handling to keep it clean and prevent contamination. Specimens are then cured in the autoclave using the layup in Figure A4 and a two hour cure cycle at 240° F with zero pressure and 28 in Hg vacuum.

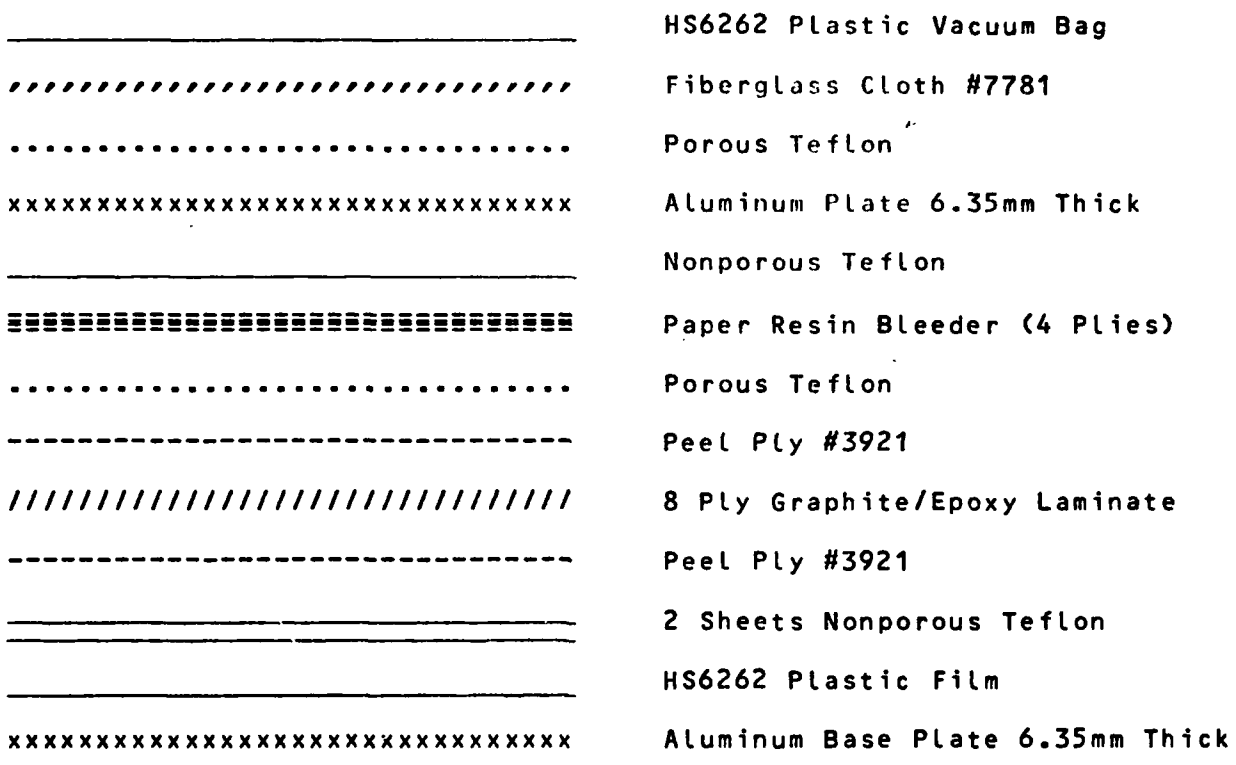

Figure A1. Curing layup for graphite/epoxy

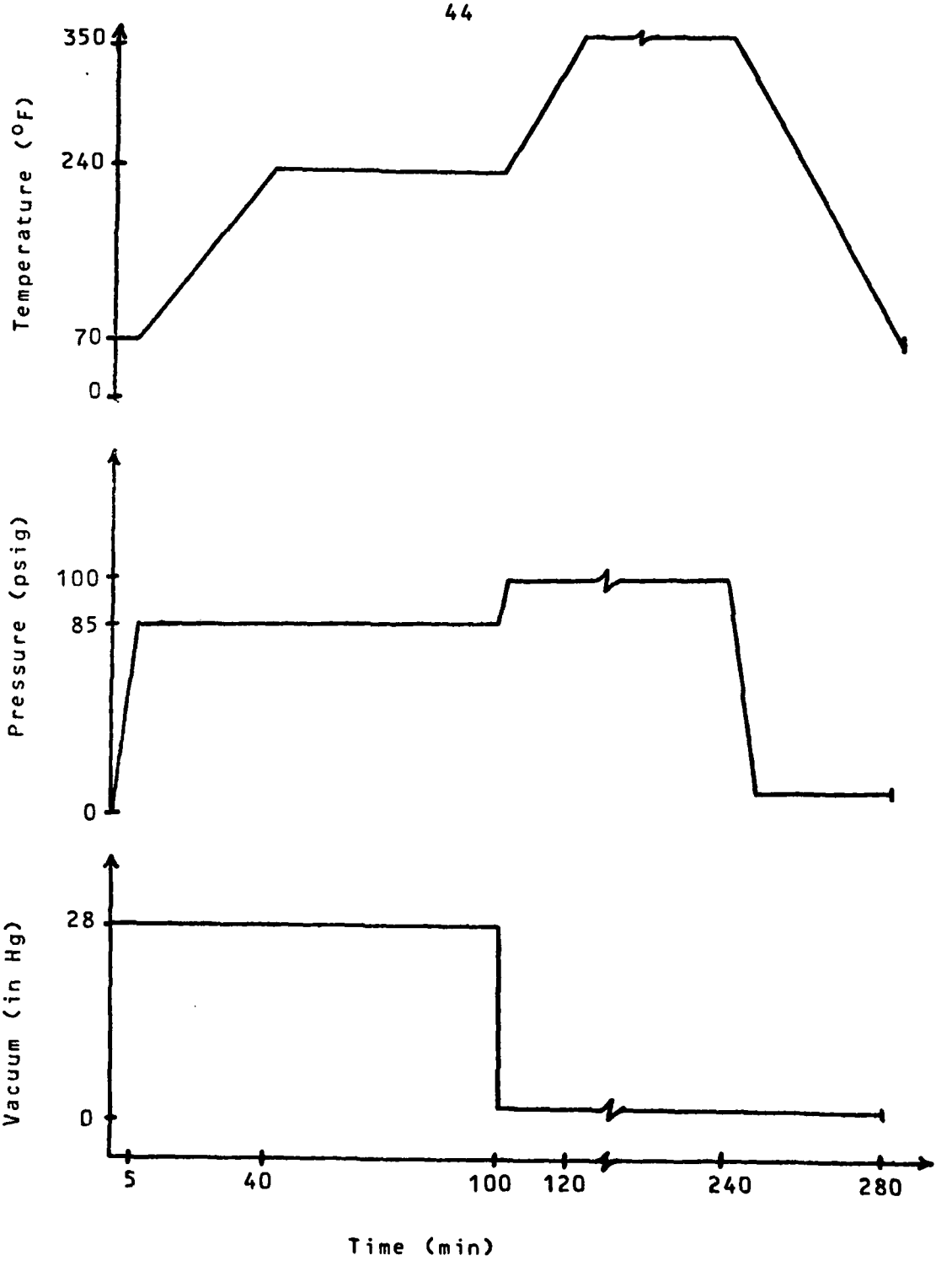

Figure A2. Curing Cycle for Graphite/Epoxy

_____	HS6262 Plastic Vacuum Bag
,,,,,,,,,,,,,,,,,,	Fiberglass Cloth #7781
xxxxxxxxxxxxxxxx	Aluminum Plate 6.35mm Thick
_____	Nonporous Teflon
==========	Fiberglass Resin Bleeder #120 (2 plies)
....	Porous Teflon
----------	Peel Ply #3921
//////////////////	8 Ply Glass/Epoxy
----------	Peel Ply #3921
....	Porous Teflon
,,,,,,,,,,,,,,,,,,	Fiberglass Resin Bleeder #120
_____	Nonporous Teflon
xxxxxxxxxxxxxxxx	Aluminum Base Plate 6.35mm Thick

Figure A3. Glass/epoxy curing layup

_____	HS6262 Plastic Vacuum Bag
,,,,,,,,,,,,,,,,,,	Fiberglass Cloth #7781
xxxxxxxxxxxxxxxx	Aluminum Plate 6.35mm Thick
_____	Nonporous Teflon
//////////////////	Specimen
_____	Nonporous Teflon
xxxxxxxxxxxxxxxx	Aluminum Base Plate 6.35mm Thick

Figure A4. Bonding layup

APPENDIX B

CRUSHING STRENGTH MAXIMUM TORQUE

The minimum bolt torque necessary to cause crushing of the graphite/epoxy between steel loading plates was calculated using beam on an elastic foundation theory (9).

Deflection in the laminate, Δt, as a function of bolt clamping force, P, modulus of the foundation, k, and distance perpendicular to load application, x, can be approximated by

$$\Delta t = \frac{P\beta}{2k} e^{-\beta x} (\cos \beta x + \sin \beta x) \qquad (B1)$$

where β is a parameter determined from the modulus of steel, E_s, of 207 GPa, and moment of inertia, I_x, using the notation

$$\beta = \sqrt[4]{\frac{k}{E_s I_x}}. \qquad (B2)$$

A value for k can be calculated by representing the transverse crushing strength, σ_c, of 172 MPa as a uniformly distributed load across the width of the plate (50.8mm), b, causing a deflection equal to the crushing strain, ε_c, of 16,120 μin/in times one half the laminate thickness (1.08mm), t. The derivation proceeds as

$$k = \frac{\sigma_c \Delta A / \Delta l}{\varepsilon_c \, t/2} = \frac{\sigma_c (b) \Delta l / \Delta l}{\varepsilon_c t/2} = \frac{2\sigma_c b}{\varepsilon_c t}. \qquad (B3)$$

Substituting this result into Eq(B2) and reducing, gives an expression for β which is dependent on the plate thickness, h,

$$\beta = \sqrt[4]{\frac{24 \nabla_c}{E_s \varepsilon_c \, th^3}} \qquad \text{(B4)}$$

For the plate thickness of 9.5mm, a value of β of .19mm^{-1} is found.

The entire width of the plate does not carry the load since the deflection goes to zero at $\beta x = 2.35$, or a distance from load application of 12mm. If the effective load carry width is taken as two-thirds this value on each side of the loading point, a new effective plate width, b_e, of 16mm is found.

Using this new width in the expression for k, Eq (B3), the critical clamping force which causes crushing,

$$\Delta t = \varepsilon_c t/2, \qquad \text{(B5)}$$

can be found by reducing Eq (B1) for the case of maximum deflection, x = 0,

$$P = \frac{2 \nabla_c \, b_e}{\beta} \qquad \text{(B6)}$$

Substituting the values given above results in a critical clamping force of 55,000 N.

Torque, T, is related to the clamping force by an equation that can be determined from the work for displacement and friction:

$$P = \frac{2\pi T}{p + 2\pi\mu D} \qquad (B7)$$

with a coefficient of friction, μ, equal to .15 for an unlubricated steel nut and bolt combination, bolt diameter, D, of 6.35mm, and fine thread pitch, p, of .91mm, the clamping force per N-m of torque is 911 N.

Using this conversion factor on the critical clamping force results in a torque of 60 N-m, which is far above the 27 N-m capability of the 6.35mm diameter cap screws.

APPENDIX C

TEST EQUIPMENT AND PROCEDURES

C.1 Static

Static testing was accomplished on the MTS 810 Hydraulic Test System. The loading fixture remained in place and each specimen was aligned perpendicular to the crosshead with a square prior to gripping and checked afterwards. The bolt was not torqued until after the alignment check. The system was operated under stroke control at a rate of .04 in/min.

C.2 Fatigue

C.2.1 Equipment

The SF-1U Mechanical Fatigue Machine with automatic static force controller and 5:1 multiplying fixture was used. The system operates at 30 Hz. Pictures of the loading grips and multiplying fixture are shown in Figures C1 and C2, respectively. Although this machine is technically outdated, it met the load increasing requirements of the Prot method and is suited to stiff materials such as graphite/epoxy.

C.2.2 Procedures

While complete instructions for operation were available, there are several aspects of test procedures that warrant discussion. The required parallel orientation of the loading fixture and specimen made it impractical to adjust loading grip length. Therefore, the specimens had to be designed so that after application of the static load, the oscillating platen and machine top plate were approximately level, as recommended by the instructions. After the specimen was put in place and bolt inserted, a load of twenty pounds was put on the specimen prior to applying torque which allowed the specimen to center bolt and pin connections with operator assistance.

The only problem with the loading fixture was a failure of the pinned connection by bolt thread crushing after fifteen runs. A bolt with a longer shaft length was substituted.

Any creep or extensions in the specimen were corrected for by the automatic static force controller, which also doubled as the prime indicator of failure. The system was sensitive to load reductions of approximately .3 percent of ultimate and impending failure in tension, shear, and corner shear were preceeded by a succession of clicks corresponding to the static motor running to correct for the slight load reductions evidenced in the static plots

(Fig 8) just prior to failure. Since bearing failure results in a load reduction of approximately five percent, the static load motor would come on for around five seconds at yield.

All step increases of static load were to the nearest whole digit (19.45 lbs) on the counter, about .75 percent of ultimate. When static and oscillating load were corrected for R value at 75 percent of static strength, the static load was reduced first by whole digits and this amount added to the oscillating load.

Although instructions called for a 30 minute static force controller warmup time, it was more on the order of two hours and worked best during long test sessions or when left on overnight.

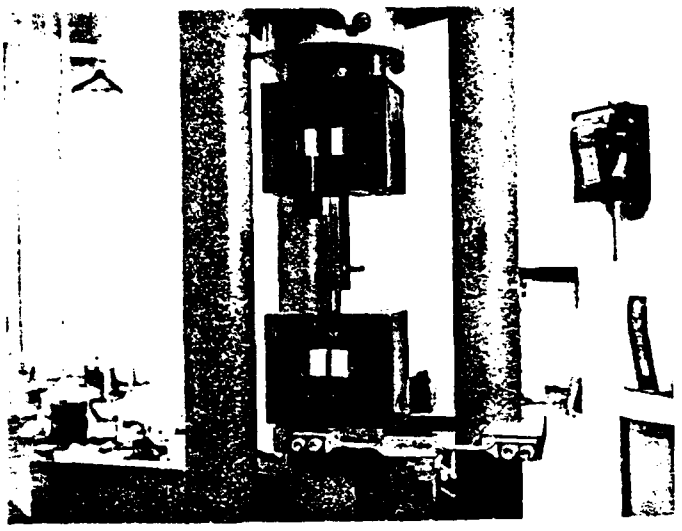

Figure C1. Fatigue Loading Grips

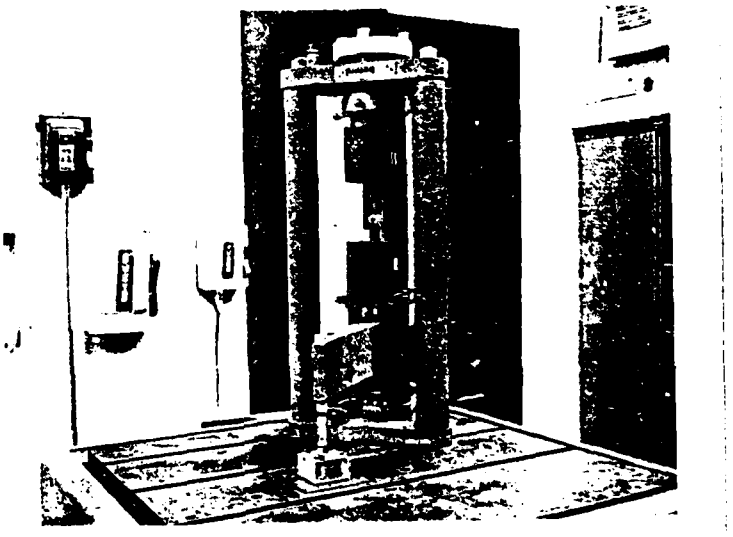

Figure C2. SF-1U 5:1 Multiplying Fixture

APPENDIX D

SPECIMEN DIMENSIONS AND FAILURE DATA

D.1 Measurements

The points used for specimen measurement of width (w), hole diameter (d), thickness (t), and edge distance (e) are shown on Figure D1.

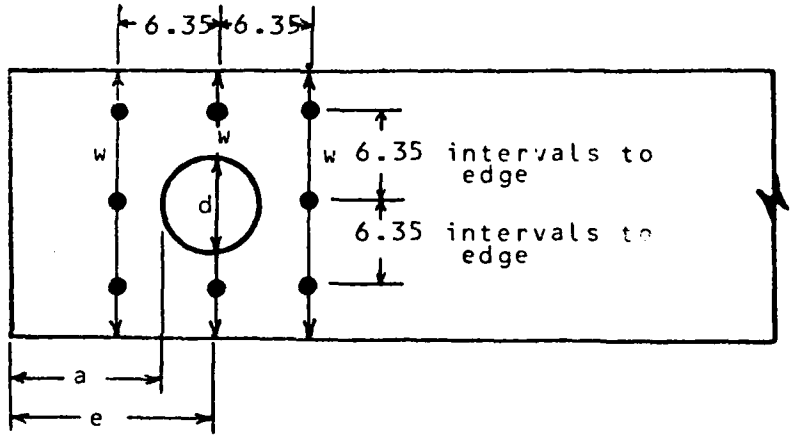

All dimensions in mm

Figure D1. Specimen measurement points

The dimensions in Tables D1 through D9 are the minimum values obtained from the three widths (w) and as many thicknesses (●) as the width would allow. Edge distance (e) was determined by measuring (a) plus one half the hole diameter (d).

Table D1

Basic Laminate-No Hole

Specimen ID	Panel Width mm	Panel Thick mm	Failure Load KNewton	Failure Mode	Tensile Strength MPascal
S180-1X	50.54	1.088	25.89	T	470.8
S280-1X	49.40	1.092	27.26	T	505.3
S380-1X	50.62	1.112	27.22	T	483.6
S180-2Y	50.54	1.090	29.45	T	534.6
S280-2Y	50.66	1.146	32.38	T	557.7

Table D2

Static Bearing And Shearout Specimens-4.0 N-m Torque

Specimen ID	Hole Diam mm	Bolt Diam mm	Panel Width mm	Edge Dist mm	Panel Thick mm	Failure Load Yld KNewton	Failure Load Ult KNewton	Failure Load	Bearing Stress Yld MPascal	Bearing Stress Ult MPascal	Tension Stress Ult MPascal	Shearout Stress Ult MPascal
S188-1A	6.38	6.27	50.70	50.29	1.114	6.45	8.89	B	923.1	1272.4	180.1	79.3
S188-1B	6.38	6.26	50.72	50.85	1.102	7.11	8.98	B	1030.0	1300.9	183.8	80.1
S188-2A	6.38	6.27	50.58	50.91	1.106	6.80	9.47	B	980.6	1365.7	193.7	84.1
S188-3B	6.40	6.27	50.64	51.36	1.100	6.94	9.52	B	1005.9	1379.9	195.6	84.3
S184-1A	6.36	6.27	50.70	25.42	1.072	5.87	7.87	B	873.0	1170.6	165.6	144.4
S184-1B	6.40	6.27	50.70	25.46	1.102	6.89	7.87	B	996.8	1138.6	161.2	140.3
S184-1C	6.36	6.27	50.72	25.52	1.072	6.36	8.45	B	946.2	1257.3	177.7	154.4
S183-1A	6.38	6.27	50.66	19.01	1.108	7.16	7.29	B/CS	1030.0	1048.7	148.6	173.1
S183-1B	6.38	6.26	50.66	19.21	1.120	6.00	7.82	B/S	855.8	1115.4	157.7	181.7
S183-1C	6.34	6.27	50.72	19.03	1.098	6.67	7.87	B/S	969.1	1143.5	160.5	188.3
S182-1A	6.40	6.27	50.70	12.92	1.042		5.29	S		809.7	114.6	196.5
S182-1B	6.40	6.27	50.66	12.88	1.062		6.13	S		920.9	130.4	224.1
S182-1C	6.34	6.26	50.70	12.41	1.098		6.32	S		919.2	129.8	231.9

Table D3

Static Bearing And Shearout Specimens-0 N-m Torque

Specimen ID	Hole Diam mm	Bolt Diam mm	Panel Width mm	Edge Dist mm	Panel Thick mm	Failure Load Yld KNewton	Failure Load Ult KNewton	Failure Mode	Bearing Stress Yld MPascal	Bearing Stress Ult MPascal	Tension Stress Ult MPascal	Shearout Stress Ult MPascal
S188-2B	6.40	6.27	50.60	51.08	1.054		3.38	B		511.6	72.6	31.4
S188-3A	6.46	6.27	50.66	50.99	1.098		3.42	B		496.6	70.5	30.5
S184-2A	6.38	6.27	50.68	25.45	1.104		3.68	B		531.5	75.2	65.5
S184-2B	6.38	6.27	50.68	25.53	1.102		3.07	B		444.6	62.9	54.6
S183-2A	6.38	6.27	50.70	18.97	1.062		3.25	B		487.9	69.0	80.7
S183-2B	6.38	6.27	50.70	19.17	1.074		3.82	B		567.5	80.3	92.8
S182-2A	6.40	6.28	50.62	12.46	1.006		2.80	B		443.5	62.9	111.7
S182-2B	6.36	6.27	50.58	12.82	1.052		3.91	B		593.0	84.1	145.0

Table D4

Static Tension Through The Hole Specimen-4.0 N-m Torque

Specimen ID	Hole Diam mm	Bolt Diam mm	Panel Width mm	Edge Dist mm	Panel Thick mm	Failure Load Yld KNewton	Failure Load Ult KNewton	Failure Mode	Bearing Stress Yld MPascal	Bearing Stress Ult MPascal	Tension Stress Ult MPascal	Shearout Stress Ult MPascal
S166-1A	6.38	6.27	38.22	38.47	1.076	5.34	6.98	B/T	791.0	1033.9	203.7	84.3
S166-1B	6.36	6.27	38.30	38.40	1.080	6.32	7.96	B/T	933.9	1176.3	230.8	96.0
S166-1C	6.36	6.27	38.34	38.10	1.038	7.03	8.23	B/T	1031.2	1207.3	236.5	99.3
S164-1A	6.36	6.27	38.22	25.50	1.094	4.69	6.18	B/T	683.5	900.7	177.3	110.8
S164-1B	6.38	6.27	38.16	25.51	1.036	5.74	6.45	B/T	883.9	993.2	195.9	122.0
S164-1C	6.38	6.26	38.24	25.27	1.045	5.69	6.89	B/T	868.4	1051.6	206.7	130.3
S162-1A	6.36	6.27	38.22	12.54	.950	4.31	4.76	B/S	723.1	798.6	157.3	199.8
S162-1B	6.38	6.27	38.26	12.99	.988	5.47	5.75	B/CS	883.0	928.0	173.7	213.1
S162-1C	6.38	6.27	38.32	12.73	.972	4.80	5.65	B/CS	788.1	927.6	182.0	228.3
S256-1A	6.38	6.27	32.28	38.01	1.022		5.78	T		901.7	218.4	74.4
S256-1B	6.36	6.27	31.98	38.40	1.000	5.70	5.87	B/T	909.1	935.6	229.1	76.4
S256-1C	6.36	6.27	31.70	38.10	.978		6.09	T		993.5	240.3	81.7
S254-1A	6.38	6.27	31.78	25.59	1.132	5.78	7.61	B/T	814.1	1071.8	264.7	136.5
S254-1B	6.36	6.27	31.80	25.58	1.170	7.43	8.41	B/T	1012.8	1146.4	282.5	140.5
S254-1C	6.36	6.27	31.84	25.58	1.178	7.12	8.85	B/T	964.3	1198.5	294.8	146.8
S252-1A	6.40	6.27	31.78	12.88	1.048		5.28	CS		804.5	198.9	196.0
S252-1B	6.38	6.27	31.74	12.81	1.068		6.00	CS		896.9	221.5	219.2
S252-1C	6.40	6.27	31.80	12.82	1.092		6.49	CS		947.9	234.0	231.8

Table D4 (Continued)

Static Tension Through The Hole Specimen-4.0 N-m Torque

Specimen ID	Hole Diam mm	Bolt Diam mm	Panel Width mm	Edge Dist mm	Panel Thick mm	Failure Load Yld KNewton	Failure Load Ult KNewton	Failure Mode	Bearing Stress Yld MPascal	Bearing Stress Ult MPascal	Tension Stress Ult MPascal	Shearout Stress Ult MPascal
S246-1A	6.38	6.27	24.84	38.37	1.126	6.29	6.67	T	890.6	944.1	320.9	77.2
S246-1B	6.36	6.26	24.86	38.28	1.114		6.76	T		968.7	328.0	79.3
S246-1C	6.36	6.26	24.86	38.14	1.090		6.14	T		898.7	304.5	73.8
S244-1A	6.36	6.27	24.84	25.54	1.112	6.09	6.89	T	872.9	987.6	335.3	121.3
S244-1B	6.38	6.27	24.88	25.39	1.128		6.32	T		893.6	302.8	108.2
S244-1C	6.36	6.27	24.90	25.32	1.084		6.67	T		982.0	331.9	121.5
S242-1A	6.38	6.27	24.98	12.77	1.080		5.47	T		807.5	272.3	198.3
S242-1B	6.38	6.27	24.96	12.87	1.138		6.27	T		878.5	296.5	214.1
S242-1C	6.38	6.27	24.94	12.75	1.098		5.78	T		839.3	283.6	206.4
S236-1A	6.38	6.27	19.42	37.71	1.024		4.27	T		664.6	319.8	55.3
S236-2A	6.36	6.27	19.24	37.52	1.174		6.49	T		881.4	429.2	73.7
S236-3A	6.38	6.27	19.32	37.57	1.132		1.20	Run Stopped		-	-	-
S234-1A	6.36	6.27	19.34	25.44	1.058		5.29	T		797.2	385.2	98.3
S234-2A	6.36	6.27	19.12	25.34	1.002		4.36	T		693.5	341.0	85.9
S234-3A	6.36	6.27	19.28	25.02	1.030		4.89	T		756.9	367.5	94.9
S232-1A	6.38	6.27	19.20	12.79	1.116		4.80	T		685.8	335.5	168.1
S232-2A	6.36	6.27	19.48	12.86	1.154		5.74	T		793.0	379.1	193.4
S232-3A	6.38	6.27	19.32	12.67	1.084		5.43	T		798.4	386.5	197.7

Table D5

Static Tension Through The Hole Specimen-0 N-m Torque

Specimen ID	Hole Diam mm	Bolt Diam mm	Panel Width mm	Edge Dist mm	Panel Thick mm	Failure Load Yld KNewton	Failure Load Ult KNewton	Failure Mode	Bearing Stress Yld MPascal	Bearing Stress Ult MPascal	Tension Stress Ult MPascal	Shearout Stress Ult MPascal
S166-2A	6.38	6.27	38.24	38.31	1.102		3.83	B		554.1	109.1	45.4
S166-2B	6.36	6.27	38.28	38.18	1.106		3.56	B		513.5	100.8	42.2
S164-2A	6.46	6.27	38.24	25.46	1.002		2.80	B		445.4	87.9	54.9
S164-2B	6.40	6.27	38.24	25.56	1.108		3.16	B		455.2	89.6	55.8
S162-2A	6.40	6.27	38.40	12.84	1.032		2.62	B		404.6	79.3	98.9
S162-2B	6.38	6.27	38.38	12.99	1.064		3.69	B		553.5	108.4	133.5
S256-2A	6.38	6.27	31.78	38.25	1.160		4.09	B		562.0	138.8	46.1
S256-2B	6.34	6.27	31.80	38.29	1.198		4.18	B		556.5	137.0	45.6
S254-2A	6.38	6.27	31.02	25.23	1.018		3.78	B		592.0	150.7	73.6
S254-2B	6.38	6.27	31.20	25.51	1.018		3.65	B		572.0	180.1	70.3
S252-2A	6.36	6.27	31.82	12.60	1.086		3.65	B		536.0	132.0	133.3
S252-2B	6.36	6.27	31.84	12.80	1.042		3.51	B		537.4	132.2	131.6
S246-2A	6.40	6.27	24.82	38.02	1.132		3.02	B		425.2	144.8	35.1
S246-2B	6.36	6.27	24.80	38.24	1.128		4.23	B		598.3	203.4	49.0
S244-2A	6.38	6.27	24.70	25.13	1.126		4.09	B		578.9	198.3	72.3
S244-2B	6.38	6.27	24.72	25.51	1.156		3.96	B		546.2	186.8	67.1
S242-2A	6.38	6.27	24.84	12.53	1.058		4.00	B		603.0	209.8	150.9
S242-2B	6.36	6.27	24.84	12.82	1.120		4.09	B		582.8	197.6	142.4

Table D5 (Continued)

Static Tension Through The Hole Specimen-0 N-m Torque

Specimen ID	Hole Diam mm	Bolt Diam mm	Panel Width mm	Edge Dist mm	Panel Thick mm	Failure Load Yld KNewton	Failure Load Ult KNewton	Failure Mode	Bearing Stress Yld MPascal	Bearing Stress Ult MPascal	Tension Stress Ult MPascal	Shearout Stress Ult MPascal
S236-4A	6.36	6.27	19.34	37.70	1.158		3.83	B		527.0	254.8	43.9
S234-4A	6.36	6.27	19.12	25.24	1.012		3.42	B		539.0	264.8	66.9
S232-4A	6.36	6.28	19.38	12.60	1.028		3.69	T		571.8	275.7	142.4

Table D6

Prot Fatigue Tension Specimens - 4.0 N-m Torque

Specimen ID	Hole Diam mm	Panel Width mm	Edge Dist mm	Panel Thick mm	Initial Stress Min MPascal	Initial Stress Max MPascal	Initial Max Stress % Static Yield	Load Rate $(Pa/Cycle)^{1/2}$	Failure Stress Min MPascal	Failure Stress Max MPascal	Final Max Stress % Static Yield	Cycles To Fail (000)
F244-1	6.36	25.68	25.70	1.146	21	141	44	46	103	312	98	61
F244-2	6.36	25.68	25.58	1.026	18	164	51	49	102	320	100	60
F244-3	6.36	25.70	25.22	.972	20	174	54	51	103	294	92	47
F244-4	6.38	25.68	25.69	1.098	17	170	53	24	84	313	98	252
F244-5	6.40	25.78	25.42	1.056	20	175	55	24	49	285	89	189
F244-6	6.36	25.80	25.58	1.052	20	174	55	24	91	326	102	257
F244-7	6.36	25.70	25.38	1.172	17	171	54	12	73	310	96	1011
F244-8	6.38	25.76	25.57	1.160	18	175	55	12	65	302	94	896
F244-9	6.38	25.68	25.45	1.096	18	170	53	12	67	297	93	838

Table D7

Prot Fatigue Shear Specimens - 4.0 N-m Torque

Specimen ID	Hole Diam mm	Panel Width mm	Edge Dist mm	Panel Thick mm	Initial Stress Min MPascal	Initial Stress Max MPascal	Initial Max Stress % Static Yield	Load Rate $(Pa/Cycle)^{1/2}$	Failure Stress Min MPascal	Failure Stress Max MPascal	Final Max Stress % Static Yield	Cycles To Fail (000)
F282-1	6.38	51.34	12.57	1.062	11	111	51	43	68	218	100	61
F282-2	6.36	51.42	12.52	1.080	11	110	51	42	74	243	112	75
F282-3	6.38	51.36	12.73	1.064	11	110	51	42	51	204	94	54
F282-4	6.36	51.36	12.70	1.092	12	113	52	21	71	227	105	258
F282-5	6.36	51.32	12.70	1.056	11	111	51	21	50	199	92	199
F282-6	6.38	51.24	12.71	1.002	11	112	51	22	42	193	89	183
F282-7	6.40	51.38	12.68	1.092	12	113	52	11	51	195	90	719
F282-8	6.36	51.36	12.88	1.114	12	113	52	10	54	208	96	863
F282-9	6.36	51.38	12.84	1.074	11	111	51	11	52	199	92	771

Table D8

Prot Fatigue Corner Shear Specimens - 4.0 N-m Torque

Specimen ID	Hole Diam mm	Panel Width mm	Edge Dist mm	Panel Thick mm	Initial Stress Min MPascal	Initial Stress Max MPascal	Initial Max Stress % Static Yield	Load Rate $(Pa/Cycle)^{1/2}$	Failure Stress Min MPascal	Failure Stress Max MPascal	Final Max Stress % Static Yield	Cycles To Fail (000)
F252-1	6.38	31.92	12.73	1.050	12	111	51	43	76	225	102	67
F252-2	6.38	32.10	12.89	1.030	12	111	51	43	79	229	104	68
F252-3	6.36	32.04	12.74	.988	12	111	51	44	86	248	112	73
F252-4	6.38	32.12	12.89	1.002	12	108	49	22	71	215	98	229
F252-5	6.36	32.04	12.90	1.022	12	112	51	21	59	211	96	211
F252-6	6.38	32.10	12.75	1.024	13	113	52	21	66	219	100	241
F252-7	6.40	32.22	12.84	1.106	12	110	50	11	55	201	92	823
F252-8	6.36	32.04	12.58	1.068	12	111	51	11	58	207	94	825
F252-9	6.36	32.10	12.54	1.108	13	113	52	11	49	200	91	768

Table D9

Prot Fatigue Bearing Specimens - 4.0 N-m Torque

Specimen ID	Hole Diam mm	Panel Width mm	Edge Dist mm	Panel Thick mm	Initial Stress Min MPascal	Initial Stress Max MPascal	Initial Max Stress % Static Yield	Load Rate $(Pa/Cycle)^{1/2}$	Failure Stress Min MPascal	Failure Stress Max MPascal	Final Max Stress % Static Yield	Cycles To Fail (000)
F388-1	6.40	51.36	51.02	1.008	49	476	49	62	318	995	103	135
F388-2	6.40	51.38	50.96	1.000	49	479	50	62	209	882	91	1048
F388-3	6.36	51.24	50.90	1.002	49	479	50	62	253	922	96	115
F388-4	6.36	51.30	51.04	1.050	51	475	49	27	267	942	98	640
F388-5	6.40	51.36	50.94	1.048	51	475	49	27	175	851	88	515
F388-6	6.38	51.40	50.81	1.038	51	478	50	27	218	897	93	574
F388-7	6.38	51.40	51.07	1.138	50	497	51	18	193	868	90	1145
F388-8	6.38	51.36	50.99	1.132	50	497	51	18	212	893	93	1222
F388-9	6.38	51.40	50.89	1.058	51	475	49	18	137	819	85	1062

APPENDIX E
FAILURE MODE PHOTOGRAPHS

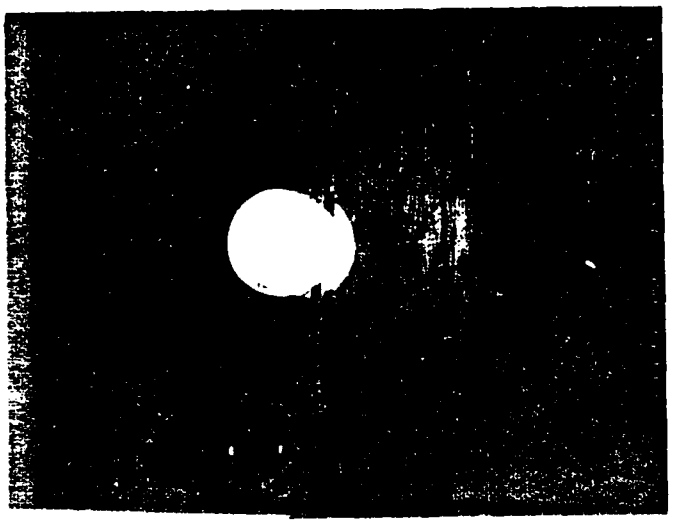

Figure E2. Bearing/Tension Failure

Figure E1. Tension Failure

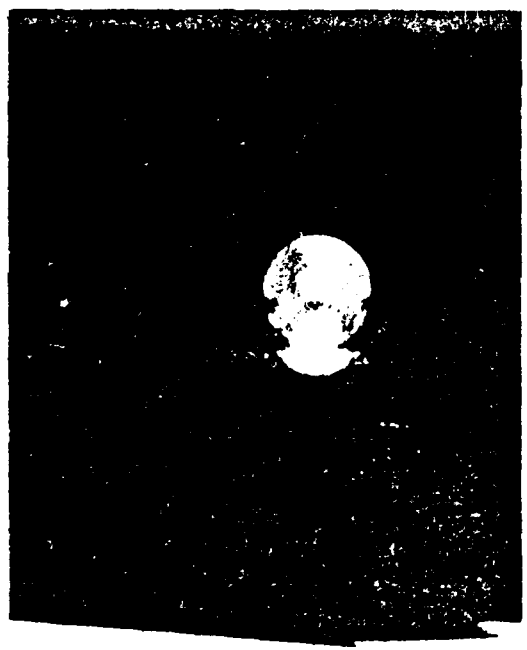

Figure E3. Bearing/Shear Failure

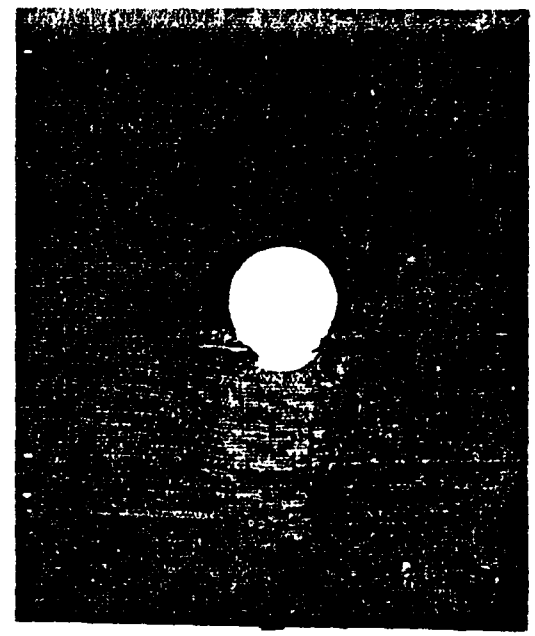

Figure E4. Bearing Failure

Figure E5. Corner Shear Failure

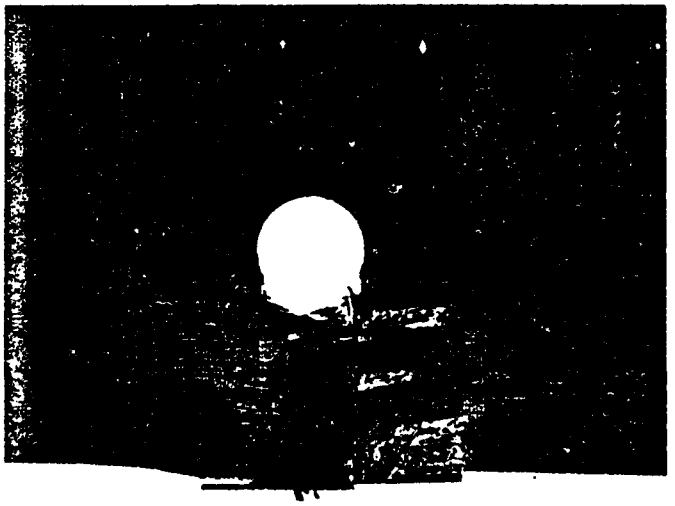

Figure E6. Shear Failure

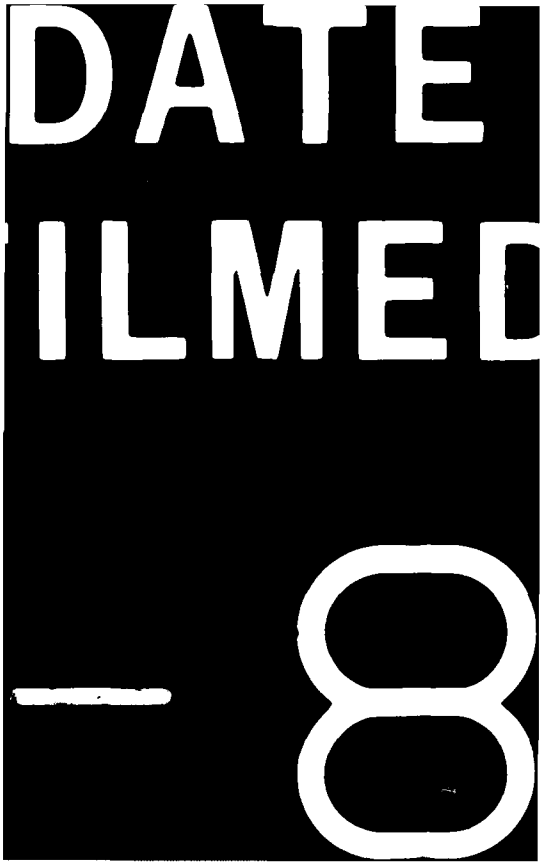
DATE
ILMED
8